

**TEA POLYPHENOL (-)EPIGALLOCATECHIN-3-GALLATE: A NEW  
TRAPPING AGENT FOR REACTIVE DICARBONYL SPECIES**

**By**

**XI SHAO**

**A thesis submitted to the**

**Graduate School-New Brunswick**

**Rutgers, The state University of New Jersey**

**In partial fulfillment of the requirements**

**For the degree of**

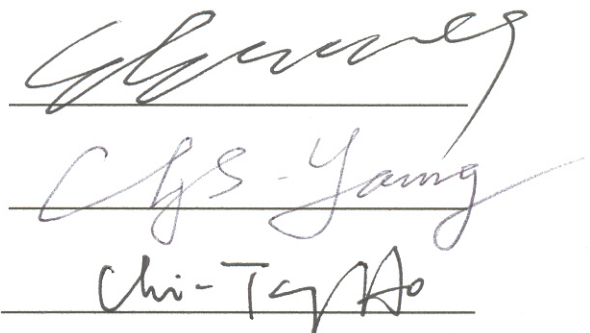
**Master of Science**

**Graduate Program in Food Science**

**Written under the direction of**

**Professor Shengmin Sang,**

**And approved by**



**New Brunswick, New Jersey**

**May, 2007**

## **ABSTRACT OF THESIS**

### **Tea polyphenol (-)Epigallocatechin-3-gallate: A new trapping agent of reactive dicarbonyl compounds**

**By XI SHAO**

**Thesis Director:**

**Professor Shengmin Sang**

Tea, made from the leaves of *Camellia sinensis*, is one of the most widely consumed beverages in the world. Many studies in humans, animal models, and cell lines suggest potential health benefits from the consumption of tea, including prevention of cancer, heart disease, and diabetes. The objective of this project is to study the trapping effect of reactive dicarbonyl compounds, the precursors of advanced glycation end products (AGEs), by tea polyphenol epigallocatechin-3-gallate (EGCG), the most abundant and major active component in tea. Previous studies have demonstrated that accumulation of reactive dicarbonyl compounds in human tissue will accelerate the vascular damage in both diabetes and uraemia. In addition, advanced glycation irreversibly and progressively modified proteins over time and yielded the AGEs. AGEs are thought to contribute to the development of diabetes mellitus and its complications. Higher levels of  $\alpha$ ,  $\beta$ -dicarbonyl compounds (e.g., glyoxal (GO) and methylglyoxal (MGO)) were observed in diabetes patients' plasma than those in healthy people's plasma. Therefore, decreasing the levels of MGO and GO will be a useful approach to prevent the development of diabetic complications. In this study, we found EGCG could trap MGO rapidly under *in vitro* conditions (pH 7.4 buffer solution, 37 °C) to form carbonyl adducts of EGCG. Two

major carbonyl adducts were purified through different column chromatography and identified by  $^1\text{H}$ ,  $^{13}\text{C}$ , and 2D NMR and MS analyses. These adducts will serve as standards for our future *in vivo* studies.

## **ACKNOWLEDGEMENTS**

I would like to take this opportunity to thank Dr. Shengmin Sang and Dr. Chi-Tang Ho for their mentoring. As a student without much previous research experience on a complicated project, Dr. Sang and Dr. Ho's close guidance makes my US transition easier and give me a lot on how carefully and seriously a scientist should do a research.

I would also like to thank my committee member, Dr Chung S. Yang, for his encouragement and valuable suggestions.

Finally, I would like to express my deep appreciation my families for their continuous encouragement and support. Without their generous love, I would not have such a great opportunity for much high value of education and working with so many great and nice people.

## TABLE OF CONTENTS

<b>ABSTRACT</b>	<b>ii</b>
<b>ACKNOWLEDGEMENTS</b>	<b>iii</b>
<b>TABLE OF CONTENTS</b>	<b>v</b>
<b>LIST OF TABLES AND ILLUSTRATIONS</b>	<b>viii</b>
<b>I. INTRODUCTION</b>	<b>1</b>
<b>1. Formation of reactive dicarbonyl compounds</b>	<b>1</b>
<b>1.1 Exogenous sources of MGO and GO</b>	<b>2</b>
<b>1.1.1 Carbohydrate</b>	<b>2</b>
<b>1.1.2 Maillard reaction</b>	<b>2</b>
<b>1.1.3 Lipid peroxidation</b>	<b>3</b>
<b>1.1.4 Microorganisms</b>	<b>3</b>
<b>1.2 Endogenous sources of MGO and GO</b>	<b>4</b>
<b>1.2.1 Enzymetic pathways</b>	<b>4</b>
<b>1.2.2 Non-enzymetic pathways</b>	<b>4</b>
<b>2. Role of reactive dicarbonyl compounds in diabetic complications</b>	<b>8</b>
<b>2.1 Carbonyl stress and AGEs formation</b>	<b>8</b>
<b>2.2 Major AGEs identified <i>in vivo</i></b>	<b>10</b>
<b>2.2.1 AGEs generated from MGO</b>	<b>10</b>
<b>2.2.2 AGEs formed from GO</b>	<b>10</b>
<b>3. Decreasing the levels of reactive dicarbonyl compounds as an effective approach to prevent the formation of AGEs</b>	<b>11</b>
<b>4. Effects of tea and its polyphenols on diabetes</b>	<b>14</b>

<b>4.1 Human study</b>	<b>15</b>
<b>4.2 Animal study</b>	<b>15</b>
<b>4.3 <i>In vivo</i> study</b>	<b>16</b>
<b>5. Effects of tea and its polyphenols on diabetes-related complications and AGEs formation</b>	<b>16</b>
<b>6. Methodologies for quantification of reactive dicarbonyl compounds</b>	<b>17</b>
<b>6.1 Sample preparation</b>	<b>17</b>
<b>6.2 Analytical methods</b>	<b>18</b>
<b>6.2.1 HPLC</b>	<b>18</b>
<b>6.2.2 GC</b>	<b>19</b>
 <b>II. HYPOTHESES AND OBJECTIVES</b>	 <b>21</b>
 <b>III. MATERIALS AND METHODS</b>	 <b>23</b>
<b>1. Development of derivatization and instrumentation methods for dicarbonyl compounds (MGO, GO) quantification</b>	<b>23</b>
<b>1.1 Derivatization method of MGO and GO</b>	<b>23</b>
<b>1.2 HPLC method for the quantifications of dicarbonyl compounds</b>	<b>23</b>
<b>1.3 Calibration</b>	<b>24</b>
<b>1.4 Recovery</b>	<b>24</b>
<b>2. Reaction conditions of EGCG and MGO <i>in vitro</i> model</b>	<b>25</b>
<b>2.1 Reactant ratio of the EGCG and MGO</b>	<b>25</b>
<b>2.2 Incubation time course study of EGCG and MGO</b>	<b>25</b>
<b>3. Developing effective method to inhibit the reaction between EGCG and MGO</b>	<b>26</b>

<b>4. Trapping of dicarbonyl compounds by EGCG</b>	<b>26</b>
<b>5. LC/ESI-MS analysis of EGCG and its MGO or GO adducts</b>	<b>27</b>
<b>6. Studying the formation of MGO or GO adducts of EGCG using LC/MS</b>	<b>27</b>
<b>7. Purification of the major mono-MGO adducts of EGCG</b>	<b>28</b>
<b>8. NMR</b>	<b>28</b>
 <b>IV. RESULTS</b>	 <b>29</b>
<b>1. Derivatization of MGO and GO with 1,2-diaminobenzene (DB)</b>	<b>29</b>
<b>2. Trapping of MGO and GO by EGCG under physiological conditions</b>	<b>29</b>
<b>3. Studying the formation of MGO or GO adducts of EGCG using LC/MS</b>	<b>30</b>
<b>4. Purification and structure elucidation of the major mono-MGO adducts of EGCG</b>	<b>32</b>
 <b>V. DISCUSSION</b>	 <b>36</b>
 <b>VI.FIGURES</b>	 <b>38</b>
<b>VII. REFERENCES</b>	<b>61</b>

## LIST OF TABLES AND ILLUSTRATIONS

<b>Table 1.</b> $\delta_H$ (400 MHz) and $\delta_C$ (100 MHz) NMR spectra data of EGCGMGO-1 and EGCGMGO-2 (CD <sub>3</sub> OD) ( $\delta$ in ppm)	<b>35</b>
<b>Figure 1.</b> Chemical structures of methylglyoxal (MGO), and glyoxal (GO)	<b>1</b>
<b>Figure 2.</b> Formation pathways of MGO	<b>6</b>
<b>Figure 3.</b> Sources of reactive dicarbonyl compounds (MGO and GO)	<b>7</b>
<b>Figure 4.</b> Cellular carbonyl represents stress as a result of glycation, lipid peroxidation, sugar autoxidation, and metabolism	<b>8</b>
<b>Figure 5.</b> Chemical structures of AGEs derived from MGO and GO	<b>11</b>
<b>Figure 6.</b> Representative advanced glycation end product (AGE) inhibitors	<b>13</b>
<b>Figure 7.</b> Chemical structures of major tea catechins	<b>14</b>
<b>Figure 8.</b> Derivatization of MGO, GO with diamino, triaminopyrimidine, PFBOA derivatives	<b>20</b>
<b>Figure 9.</b> Formation of ascorbyl adducts from dehydroascrobic acid and EGCG	<b>22</b>
<b>Figure 10.</b> Sample preparation, incubation conditions, and derivatization procedure	<b>38</b>
<b>Figure 11.</b> Formation of Methylquinoxaline and Quinoxaline	<b>39</b>
<b>Figure 12.</b> Time course of the derivatization of MGO with 1,2-diaminobenzene (DB) under physiological conditions (37°C, pH 7.4)	<b>40</b>
<b>Figure 13.</b> Time course of the derivatization of GO with 1,2- diaminobenzene (DB) under physiological conditions (37°C, pH 7.4)	<b>41</b>
<b>Figure 14.</b> The effect of pH on derivatization of MGO with 1,2- diaminobenzene (DB) at 37°C	<b>42</b>



<b>Figure 15.</b> Trapping of MGO and GO by EGCG under physiological conditions (37 °C, pH 7.4)	<b>43</b>
<b>Figure 16.</b> The effect of pH on the trapping of MGO by EGCG at 37°C	<b>44</b>
<b>Figure 17.</b> LC total ion chromatograms of EGCG after incubation of different ratio of MGO (3:1, 1:1, and 1:3) for 60 min	<b>45</b>
<b>Figure 18.</b> LC total ion chromatograms of EGCG after incubation of different ratio of GO (3:1, 1:1, and 1:3) for 60 min	<b>46</b>
<b>Figure 19.</b> LC/MS/MS spectra of mono-MGO adducts of EGCG	<b>47</b>
<b>Figure 20.</b> LC/MS/MS spectra of mono-GO adducts of EGCG	<b>48</b>
<b>Figure 21.</b> LC/MS/MS spectra of di-MGO adducts of EGCG	<b>49</b>
<b>Figure 22.</b> LC/MS/MS spectra of di-MGO adducts of EGCG	<b>50</b>
<b>Figure 23.</b> Formation of the mono-MGO adducts of EGCG	<b>51</b>
<b>Figure 24.</b> <sup>1</sup> H-NMR spectrum of EGCGMGO-1	<b>52</b>
<b>Figure 25.</b> <sup>13</sup> C-NMR spectrum of EGCGMGO-1	<b>53</b>
<b>Figure 26.</b> HMBC (Heteronuclear Multiple Bond Correlation) spectrum of EGCGMGO-1	<b>54</b>
<b>Figure 27.</b> Significant HMBC (H→C) correlations of EGCGMGO-1 and EGCGMGO-2	<b>55</b>
<b>Figure 28.</b> HMQC (Heteronuclear Multiple Quantum Correlation) spectrum of EGCGMGO-1	<b>56</b>
<b>Figure 29.</b> <sup>1</sup> H-NMR spectrum of EGCGMGO-2	<b>57</b>
<b>Figure 30.</b> <sup>13</sup> C-NMR spectrum of EGCGMGO-2	<b>58</b>
<b>Figure 31.</b> HMBC (Heteronuclear Multiple Bond Correlation) spectrum of EGCGMGO-2	<b>59</b>
<b>Figure 32.</b> HMQC (Heteronuclear Multiple Quantum Correlation) spectrum of	



## Introduction

### 1. Formation of reactive dicarbonyl compounds

The reactive dicarbonyl compounds, for example, methylglyoxal (MGO) and glyoxal (GO), also named as  $\alpha$ -Oxoaldehyde,  $\alpha$ ,  $\beta$ -diketone, have been widely concerned because they are highly reactive and readily form adducts with biological substances such as proteins, phospholipids, and DNA. Either the bioactive dicarbonyl compounds themselves or adducts generated by them result in several health issues, especially in relation to the complications of diabetes (*Beisswenger and Szwegold, 2003*).

Generally, the exogenous sources of reactive dicarbonyl compounds include food products, beverages, water, and cigarette smoke (*Nemet and Turk, 2006*). The endogenous reactive carbonyl compounds are produced both by enzymatic and nonenzymatic pathways.

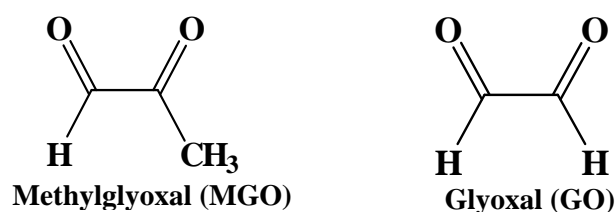


**Figure 1.** Chemical structures of methylglyoxal (MGO), glyoxal (GO).

## **1.1 Exogenous sources of MGO and GO**

The exogenous sources of MGO and GO are formed by carbohydrate auto-oxidation and degradation, Maillard reaction, lipid peroxidation, and microorganisms during industrial processing, cooking, or prolonged storage (*Nicholl and Bucala, 1998*).

### **1.1.1 Carbohydrate**

MGO and GO are produced through degradation of sugar moiety by retro-aldol condensation (Wolf pathway) and auto-oxidation from carbohydrates. Transition metal, such as  $\text{Cu}^{2+}$  and  $\text{Fe}^{2+}$ , can provide catalytic sites for this process (*Yim et al., 2001*). The fragmentation procedure is affected by both alkaline conditions and food processing. Further, previous study showed that the yields of MGO from monosaccharides are much higher than those from disaccharides while heated (*Hollnagel and Kroh, 1998*), suggesting that the formation of MGO and GO is also affected by the sugar species.

### **1.1.2 Maillard reaction**

MGO and GO are formed in different steps of the Maillard reaction. In early glycation, MGO and GO are generated from Schiff base through Namiki pathway. In advanced glycation, Amadori products induce the formation of MGO and GO through a serious complicated rearrangement (*Thornalley, 2005*). The reaction conditions, such as temperature will influence the formation of MGO and GO in the Maillard reaction. For example, glycine and  $\beta$ -alanine mixture was heated under various temperatures;

the effect of temperature on MGO production is significant since the yields of MGO increased almost two folds when the reaction temperature increased from 100°C to 120°C (*Marins et al., 2003*).

### **1.1.3 Lipid peroxidation**

The oxidative degradation of different lipids can produce MGO and GO in food that is in storage or processing. Previous studies have demonstrated the formation of MGO and GO in different lipid origins: tuna, soybean, olive, and corn oils under accelerated storage conditions (60°C for 3 and 7 days) or cooking (200°C for 1h) (*Fujioka and Shibamoto, 2004*). There are three proposed mechanisms of lipid peroxidation: auto-oxidation by free radical reaction, photo-oxidation, and enzyme action. Besides the third one, reactive oxygen species (ROS), as initiators, play an important role in other two lipid peroxidation pathways (*Halliwel and Chirico, 1993*).

### **1.1.4 Microorganisms**

Accumulation of MGO and GO occurs in the growth medium of microorganisms during many fermentation processes, such as wine or milk. In wine, the formation of MGO in alcoholic fermentation is induced by *Saccharomyces cerevisiae* (Revel et al., 2000). In milk, the generation of MGO occurs during milk fermentation because of *Lactobacillus* sp. (*Bednarski et al., 1989*). Further, MGO is formed in living organisms during the physiological process taking place in several plants, for instance,

rice, mustard, and tobacco.

## **1.2 Endogenous sources of MGO and GO**

*In vivo*, the MGO and GO can be produced by either enzymatic or non-enzymatic pathways.

### **1.2.1 Enzymetic pathways**

The enzymatic pathways represent a series of reactions which are catalyzed by three kinds of enzymes: methylglyoxal synthase, amine oxidase(s), and cytochrome P450 IIE1 isozyme(s). Methylglyoxal synthase catalyzes the transformation of dihydroxyacetone-phosphate (DHA-P) into MGO. And the catabolism of proteins via aminoacetone mediated with amine oxidase can also produce MGO (*Lyles and Singh, 1992*). Enzymatic oxidations of ketone bodies (acetoacetate and acetone) induce the generation of MGO via the catabolism of acetol by cytochrome P450 IIE1 isozyme(s) (*Casazza et al., 1984*).

### **1.2.2 Non-enzymetic pathways**

The non-enzymatic pathways of MGO generation include decomposition of DHA-P, the Maillard reaction, oxidation of acetol, and lipid peroxidation (*Kalapos, 1999*).

One of the most important production pathways of MGO occurs from the triose phosphate intermediates in the glycolytic pathway (**Figure. 2**), which includes

dihydroxyacetone phosphate (DAP) and glyceraldehydes 3-phosphate (GA3P). MGO is generated by two processes: (1) a spontaneous non-enzymatic elimination of the phosphate group, (2) decomposition of an ene-diol triose phosphate intermediate that 'leak' from the active site of triose phosphate isomerase (*Pompliano et al., 1990; Richard, 1993*). The following scheme represents these pathways.

Compare with the origin of MGO, the pathways of GO formation are poorly understood. Much of our understanding of GO is formed from oxidative fragmentation of Schiff's base, glucose auto-oxidation and degradation, lipid peroxidation, and fructose-phosphate fragmentation.

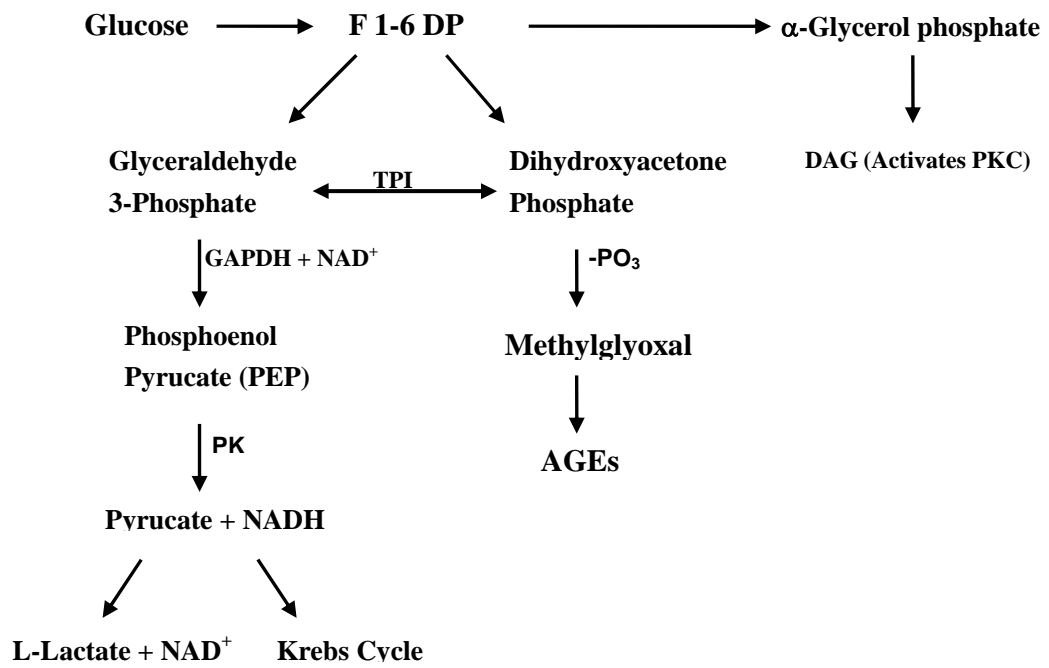


**Figure 2.** Pathways for producing MGO [1]

F 1-6 DP, fructose 1,6- diphosphate; TPI, triose phosphate isomerase; DAG, diacylglycerol; PKC, protein kinase C; PK, pyruvate kinase; LDH, lactate dehydrogenase; FN3K, fructosamine 3-kinase.



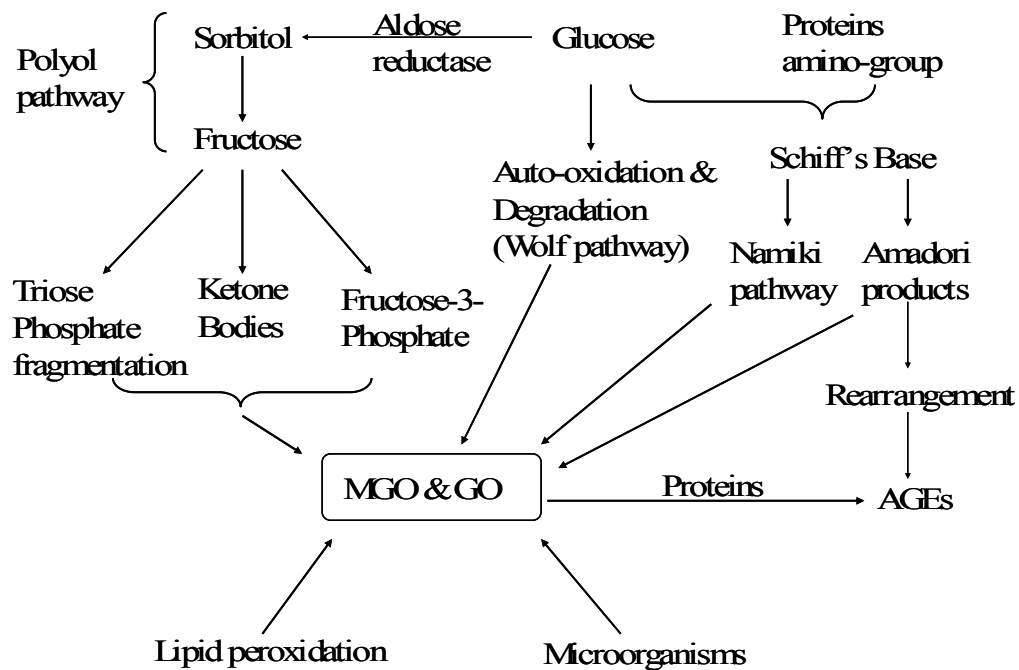


**Figure 3.** Sources of reactive dicarbonyl compounds (MGO and GO) (*Singh et al., 2001*).

## 2. Role of reactive dicarbonyl compounds in diabetic complications

Advanced glycation irreversibly and progressively modifies proteins and generates the Advanced glycation end-products (AGEs). AGEs are thought as a reason to develop diabetic complications. The accumulation of reactive dicarbonyl compounds (e.g. MGO and GO) *in vivo* is termed as “carbonyl stress” which plays a significant role in the generation of AGEs (**Figure 4**).

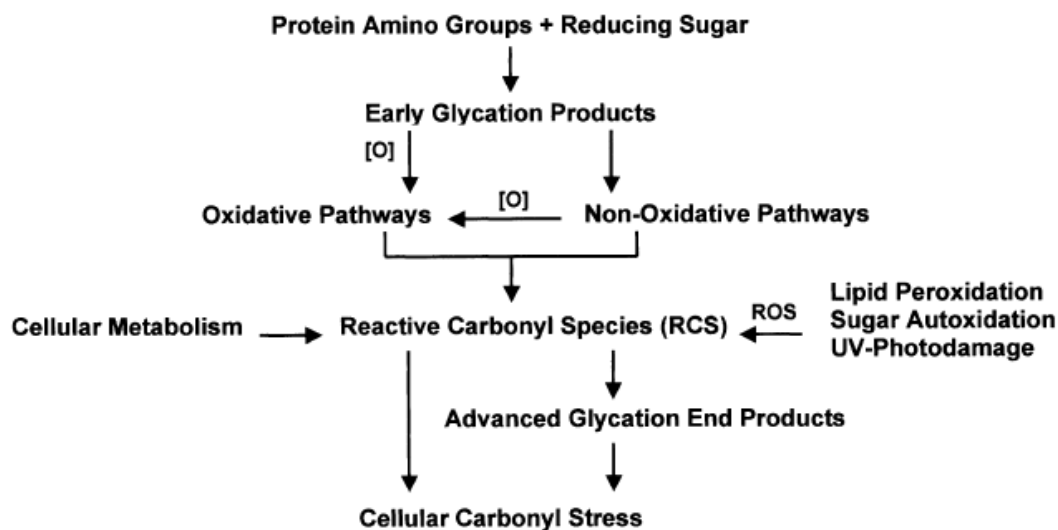


**Figure 4.** Cellular carbonyl represents stress as a result of glycation, lipid peroxidation, sugar autooxidation, and metabolism. Oxygen-dependent and –independent pathways lead to the formation of various reactive carbonyl species, including  $\alpha$ -dicarbonyls, as a key that intermediates for the accumulation of protein damage (Miyata *et al.*, 1996).

## 2.1 Carbonyl stress and AGEs formation

MGO, GO, and other reactive carbonyl compounds formed from both glycooxidation and lipoxidation sources and the subsequent carbonyl modification of proteins is called “carbonyl stress” (Golej *et al.*, 1998; Miyata *et al.*, 2000), which is a highlighted phenomenon speeded up in diabetic complications. Recently, the carbonyl stress hypothesis underlines the functions of reactive dicarbonyl compounds to modify pathogenic protein, lipid, and DNA and form toxin adducts AGEs.

The formation of AGEs is a complex process in which reducing sugar (e.g., glucose) and proteins are employed as the precursors. The initial reaction between a carbonyl group of the reducing sugar and a free amino group of proteins lead to the formation of fructosamines via a Schiff's base by classic Amadori rearrangement (*Singh et al., 2001*). Then, several reactive dicarbonyl compounds, such as MGO and GO, are formed from Schiff's base and Amadori products by a series of reactions. New formed reactive dicarbonyl compounds further modify proteins to generate AGEs of various chemical structures (*Creighton and Guha, 1988; Barrensheen and Braun, 1931*).

Once AGEs were formed, they can only degrade when the precursor proteins degraded. The most extensive accumulation of AGEs occurs in tissues that contain long-lived proteins, such as crystalline in the lens and collagen in the extracellular matrix of connective tissues (*Michael et al., 2003*). AGEs can either interfere with physical and chemical properties of proteins or cellular processes. For instance, the accumulation of AGEs decreases the collagen turnover and, thereby, renders particular cartilage tissues more prone to mechanical damage (*DeGroot et al., 2001*). The accumulation of AGEs is promoted in patients with diabetes. Formation of AGEs increases at a greater rate than the increase in blood glucose; this suggests that even moderate elevations in diabetic blood glucose levels result in substantial increases in AGEs accumulation (*Jakus and Rietbrock, 2004; Gugliucci, 2000*).

## 2.2 Major AGEs identified *in vivo*

MGO and GO are two major dicarbonyl compounds found in humans. Especially in patients with insulin-dependent and non-insulin dependent diabetes, the level of MGO was 2-6 folds higher than those of healthy people (*Odani et al., 1999*). The MGO and GO are extremely reactive and easily modify lysine, arginine, and cysteine residues on proteins (*Nagaraj et al., 2002*). Several dicarbonyl-derived products *in vivo* have been identified.

### 2.2.1 AGEs generated from MGO

So far, several AGEs derived from MGO *in vivo* have been identified. The most common measured AGE *in vivo* was methylglyoxal-lysine dimer (MOLD), which is formed from the reaction of methylglyoxal derivative with two lysine residues (*Brunner et al., 1998*). Moreover, Aminoimidazoline imine cross-link was thought to be derived from reaction of arginine and an  $\alpha$ -oxoaldimin Schiff base of a lysine residue and MGO (*Lederer and Klaiber, 1999*). The reaction of MGO with the guanidine group of arginine can also lead to formation of AGEs called imidazolone (*Paul et al., 1998*). Carboxyethyllysine (CEL) derived from MGO is found in proteins and in free form *in vivo* (*Hakim et al., 2003*).

### 2.2.2 AGEs formed from GO

Under physiological conditions, several AGEs can also be generated by GO, such as CML (carboxymethyllysine), GOLD (glyoxal-lysine-dimer), imidazolone, or

Aminoimidazoline imine cross-link. The chemical structures of AGEs derived from both MGO and GO are shown in **Figure 5**.

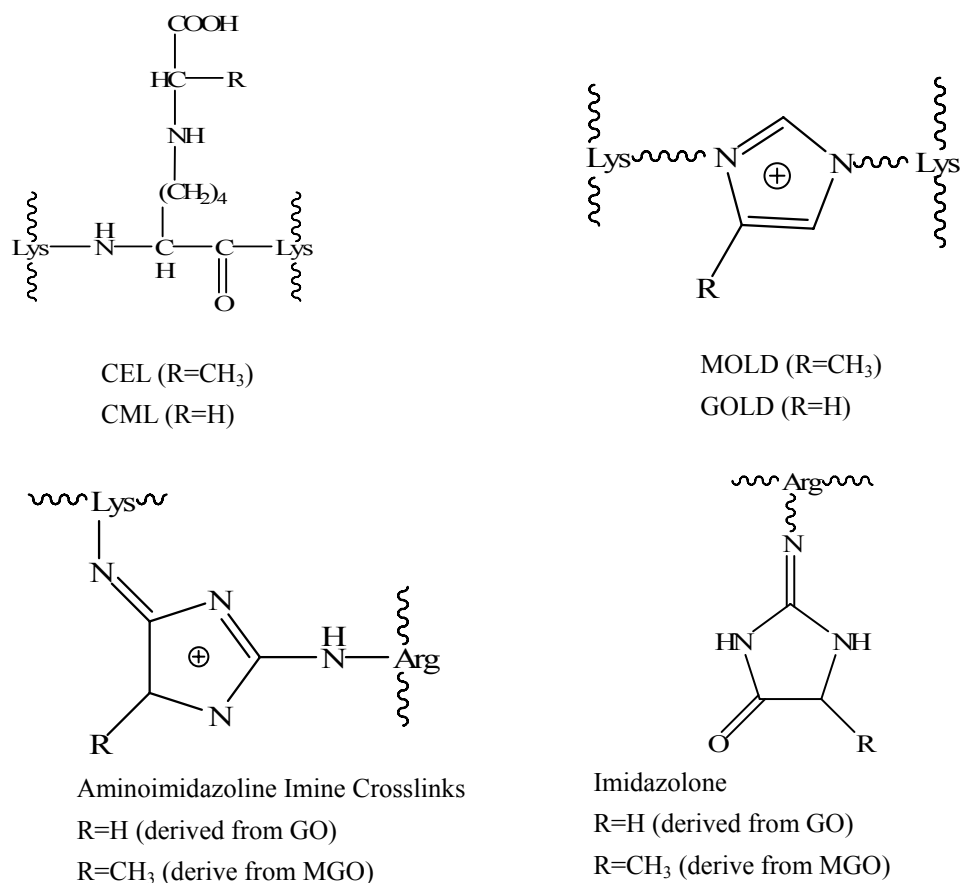


**Figure 5.** Chemical structures of AGEs derived from MGO and GO.

### 3. Decreasing the levels of reactive dicarbonyl compounds as an effective approach to prevent the formation of AGEs

The accumulation of AGEs in tissues and organs has been widely discussed as an important factor of developing diabetic complications, such as retinopathy, nephropathy, neuropathy, and macrovascular disease atherosclerosis (*Bucala and*

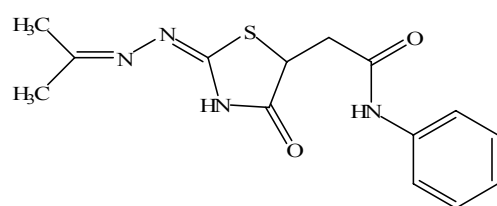
*Vlassara, 1995; Vlassara, 1995; Gugliucci, 2000; Jakus and Rietbrock, 2004*). To lower the level of AGEs in physiological condition by suppressing the reactive dicarbonyl compounds would be an effective approach to prevent the formation of AGEs.

Aminoguanidine (Pimagedine) was the most well-known AGE inhibitor discovered in 1986 (*Bolton et al., 2004*). Aminoguanidine quenches toxic reactive dicarbonyl compounds by form the corresponding adducts, 3-amino-1,2,4-triazines, relatively non-toxin compound (*Lo et al., 1994*). In animal study, the prevention of AGEs formation by aminoguanidine delays evolving the microvascular lesions in diabetic animals (*Edelstein and Brownlee, 1992*). Although Aminoguanidine performed very well on suppressing AGE formation, the drug is not being further advanced because of the side effects in phase III clinical trials in patients with diabetes (*Stadler et al., 2005*).

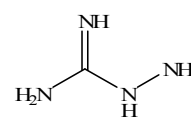
Metformin as an oral antihyperglycemic agent is usually used for the management of non-insulin-dependent diabetes mellitus (NIDDM). The trapping of MGO and GO by metformin was studied by *Daniel and Nicolas in 1999*. Their research strongly suggested that metformin can effectively quench MGO and GO to form subsequent adducts: triazepinoe and non-methylated trazepinoe under in vitro condition. More recently, *Beisswenger and Ruggiero-Lopez* further proved the scavenging effect of metformin by decreasing the MGO level *in vivo* (*Beisswenger and Ruggiero-Lopez,*

2003).

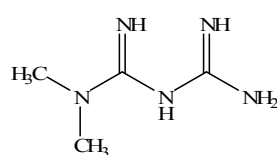
In addition, several other potential drug candidates have been tested on AGE inhibition by sequestering reactive dicarbonyl compounds, such as pyridoxamine (Pyridorin<sup>®</sup>) and 4-oxo-N-phenyl-4,5-dihydro-2-[(1-methylethylidene)hydrazino]-5-thiazoleacetamide (OPB-9195). The chemical structures are showed in **Figure 6** (Bolton *et al.*, 2004)



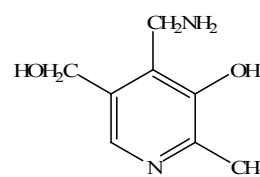
OPB-9195



Aminoguanidine



Metformin



Pyridoxamine

**Figure 6.** Representative advanced glycation end product (AGE) inhibitors [41].

#### 4. Effects of tea and its polyphenols on diabetes

Tea as the most widely consumed beverage in the world is believed to have medicinal efficacy in the prevention and treatment of diabetes. Tea polyphenols also known as catechins are considered to be diabetes chemopreventative agents. The major polyphenols in green tea include (-)-epicatechin (EC), (-)-epigallocatechin (EGC), (-)-epigallocatechin gallate (EGCG), and (-)-epicatechin-3-gallate (ECG) (**Figure 7**).

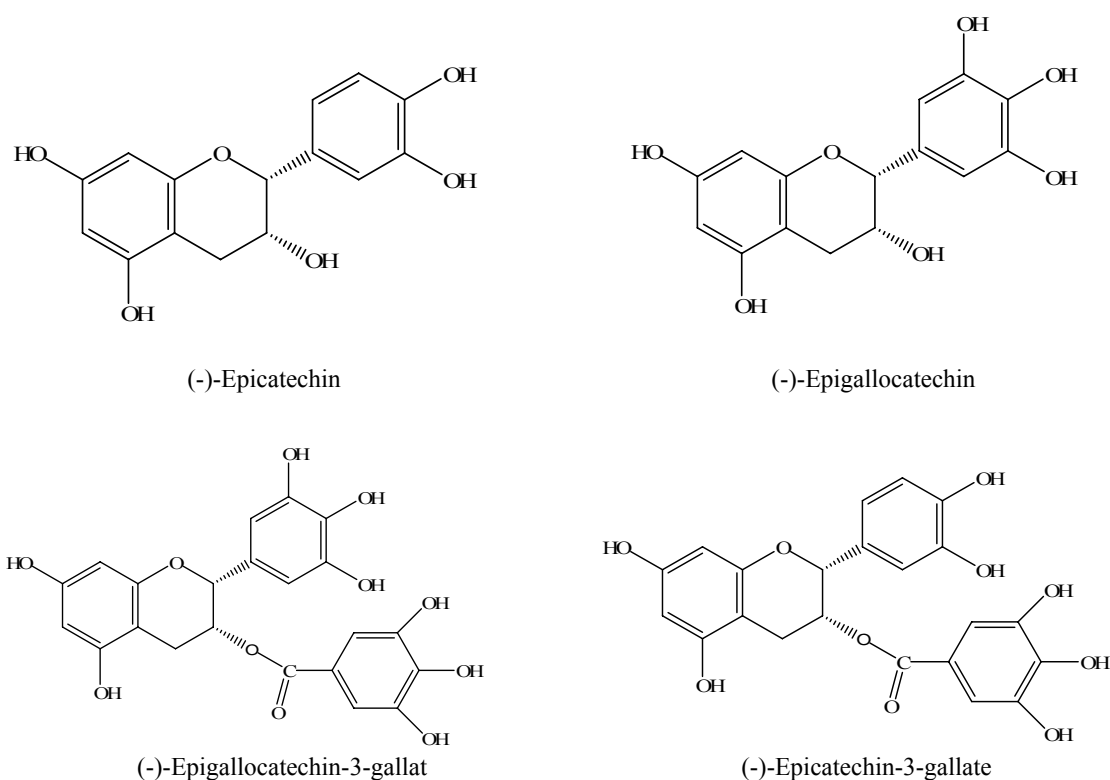


**Figure 7.** Chemical structures of some major tea polyphenols (Yang *et al.*, 1997).



#### **4.1 Human study**

The effects of tea on diabetes have received increasing attention as human studies' data accumulated. A recent study suggested that green tea promotes glucose metabolism in healthy humans in oral glucose tolerance tests (*Hiroshi et al., 2004*). Antihyperglycemic effect of oolong tea has been tested in human study: compared with water control group, plasma glucose and fructosamine levels of type 2 diabetes patients decreased significantly after daily consumption of oolong tea (*Kazuaki et al., 2003*). Black tea is known as a fermented tea which contains more catechins condensation products. Epidemiological evidences indicated that the increased black tea consumption would significantly decrease levels of serum glucose (*Hakim et al., 2003*).

#### **4.2 Animal study**

Several animal studies have shown that tea and tea polyphenols had potential anti-diabetes effect. For instance, the significant reductions of serum glucose were observed in EGCG-treated Sprague-Dwley rats, male lean and obese Zucker rats (*Hakim et al., 2003*). Moreover, daily treatment of green tea to rats with streptozotocin (STZ)-induced diabetes showed inhibition of diabetic cataracts by lowering plasma and lens glucose levels. The same phenomenon was noted in a black tea treatment group (*Natsuki et al., 1993*). Finally, green tea lowered blood glucose concentrations in the genetically diabetic db/db mice 2-6 h after administration at 300 mg/kg bw; whereas, no effect was observed in control mice (*Hiroshi et al., 2004*).

### 4.3 *In vivo* study

The reduction of carbohydrate absorption from the intestine of rats with a saccharide-supplemented by EGCG or green tea is based upon suppression of the activity of intestinal  $\alpha$ -amylase, sucrase, or  $\alpha$ -glucosidase (*Natsuki et al., 1993*). Also, green tea enhances insulin sensitivity of normal and fructose-fed rats as demonstrated by increased glucose uptake by muscle cells (*Ahmed et al., 1986*).

## 5. Effects of tea and its polyphenols on diabetes-related complications and AGEs formation

The ability of preventing diabetic-related complications by tea and its polyphenols has been tested in several studies. For instance, oral administration of tea catechins retarded the progression of functional and morphological changes in the kidney of STZ-induced diabetic rats (*Michiyo et al., 2006*). Also, the effects of ameliorating glucose toxicity, renal injury, and thus alleviating renal damage by EGCG have been pointed out in diabetic nephropathy model rats (*Yamabe et al., 2006*).

The detailed mechanisms for the prevention of diabetic complications by tea and its polyphenols are remaining for further studies. Several studies showed that those effects could partially because of the inhibition of AGEs formation. *Rutter et. al.* reported that green tea extract was able to delay collagen aging in C57Bl/6 mice by blocking AGEs formation and collagen cross-linking (*Rutter et al., 2003*). In addition, EGCG showed effects of reducing renal AGEs accumulation and its related protein

expression in the kidney cortex based upon STZ-induced diabetic nephropathy model rats [50]. In vitro study, *Lai et al.* demonstrated green tea polyphenols dose-dependently inhibited AGE-stimulated proliferation and p44/42 mitogen-activated protein kinase (MAPK) expression of rat vascular smooth muscle cells (VSMCs) (*Ping et al., 2004*).

Meanwhile, tea polyphenols may inhibit the formation of AGEs by trapping reactive dicarbonyl compounds. A recent study explored the inhibitory effect of tea polyphenols, including catechins, EC, ECG, EGC, EGCG, on different stages of protein glycation including MGO-mediated protein glycation (*Wu et al., 2005*). EGCG exhibited significant inhibitory effects on MGO-mediated protein glycation by 69.1%.

## **6. Methodologies for quantification of reactive dicarbonyl compounds**

### **6.1 Sample preparation**

Since the insolubility of proteins during chromatographic analysis and the necessity of the reversibly bound MGO liberation from proteins, protein precipitation plays a significant role in MGO quantification process. Perchloric acid (PCA) is widely used in the protein precipitation procedure because of the low pH that would prevent degradation of dihydroxyacetone phosphate and 3-phosphate to MGO through phosphate elimination (*Nemet et al., 2006*). However, PCA can increase MGO level due to oxidative degradation of nucleic acids to MGO in biological samples, thereby

causes inaccurate quantification (*Chaplen et al., 1996*). Since Trifluoroacetic acid (TFA) could easily be removed by evaporation or freeze drying, which is often used for deproteinization of human plasma samples. In addition, deproteinization with methanol is not recommended because of the large solvent volumes and extended periods of time requirements (*McLellan et al., 1992*).

## **6.2 Analytical methods**

### **6.2.1 HPLC**

Since MGO can not be directly measured, most of HPLC methods for quantification are based on MGO derivatization into quinoxaline adducts with diamino derivatives of benzene or naphthalene. These quinoxaline can easily be monitored either by UV detector at 300-360 nm or by fluorescent detector with excitation wavelengths at 300-360 nm and emission wavelength at 380-450 nm (*Nemet et al., 2004*).

HPLC method where MGO was derivatized into the corresponding fluorescent pteridine derivative with 6-hydroxy-2,4,5-triaminopyrimidine (TRI) or 2-ace-trlthiazolidine by cysteamine have also been described. The main disadvantage is that the new derivatization can form two kinds of isomers for MGO and affect the accurate of quantification (*Espinosa et al., 1998*).

More recently, electrospray ionization liquid chromatography/mass spectrometry (ESI/LC/MS) method has been developed based upon the quantification of dicarbonyl

adducts with 2,3-diaminonaphthalene. This method offers the advantage of greater specificity for measuring dicarbonyl compounds (*Randell and Vasdev, 2005*). However, this method requires time-consuming liquid-liquid or solid-phase extraction (SPE) and considerable quantities of highly pure, usually toxic, organic solvents.

Generally, injection of the sample to the instrumentation would be the last step of MGO quantification. However, the concentration of MGO in samples might be too low to measure. So the pre-concentration of the sample is often necessary. Usually, the liquid-liquid extraction and SPE will be used and later followed by evaporation of organic solvent or freeze-drying. HPLC analysis was usually performed on the reverse phase C<sub>18</sub> columns and eluted with water solutions of acids or buffers in combination with methanol or ACN under gradient or isocratic conditions.

### **6.2.2 GC**

GC methods were relied on MGO derivatization by 1,2-diaminobenzene (OPD) with detection either on MS/SIM or on specific nitrogen phosphorus detector (NPD), and by o-(2,3,4,5,6-pentafluorobenzyl) hydroxylamine hydrochloride (PFBOA) detection either on MS/SIM detector, electron-capture detector (EDC), NPD, or flame photometric detector (*Annunziata et al., 2003*). The development of GC method offers the advantage of applying less sample treatment and low-price equipment to perform highly specific measurements. The time-consuming extraction process and toxic, organic solvents application is considered to be the disadvantages of GC method. The

GC analysis is usually performed on fused-silica capillary columns with He as carrier gas.

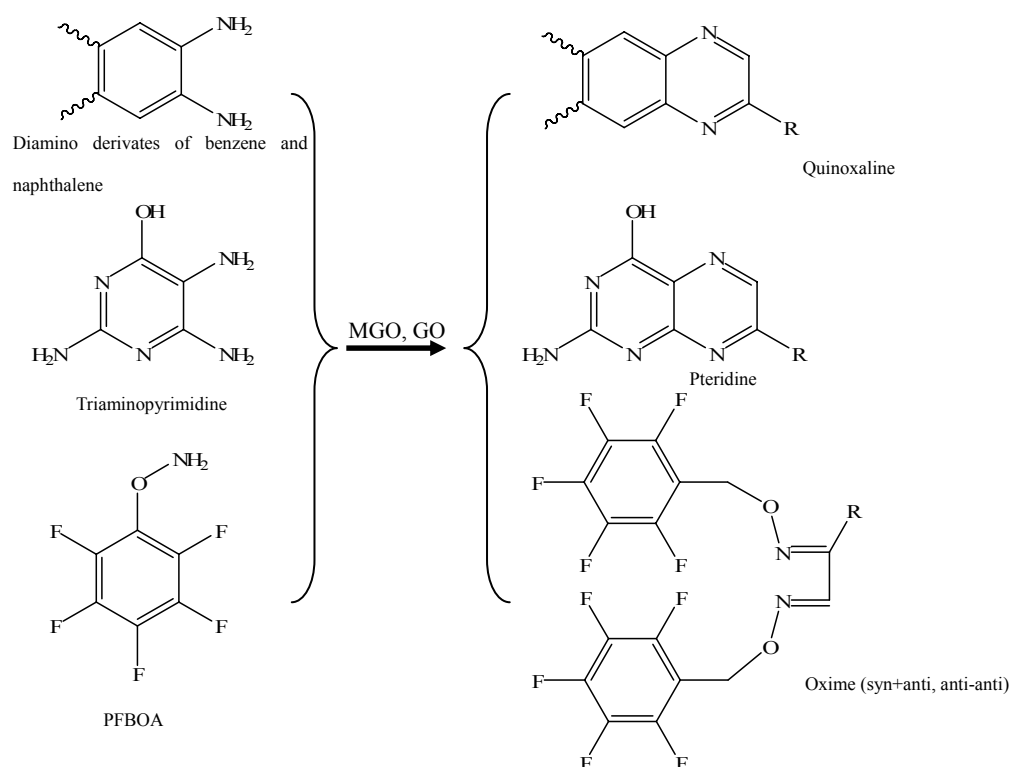


**Figure 8.** Derivatization of MGO, GO with diamino derivatives of benzene and naphthalene, triaminopyrimidine, and PFBOA (*Espinosa-Mansilla et al., 1998*).

## Hypothesis

To lower the level of dicarbonyl compounds would suppress the formation of AGEs and thereby prevent the development of diabetic complications. While tea consumption has been shown to decrease the glucose level in physiological conditions, to scavenge the reactive oxygen species (ROS) and further prevent the generation of reactive carbonyl species (RCS). Moreover, Dr. Sang's unpublished data have shown that EGCG can efficiently react with dehydroascorbic acid, which has the dicarbonyl structural features to form related ascorbyl adducts (**Figure 9**). Thus, our hypothesis is that tea catechins, such as EGCG, can trap the reactive dicarbonyl compounds (e.g. MG and GO) and thereby suppress the formation of AGEs and the development of carbonyl stress.

## Research objectives

1. To study the trapping of reactive dicarbonyl compounds by EGCG.
2. To purify and identify the major MGO adducts of EGCG.

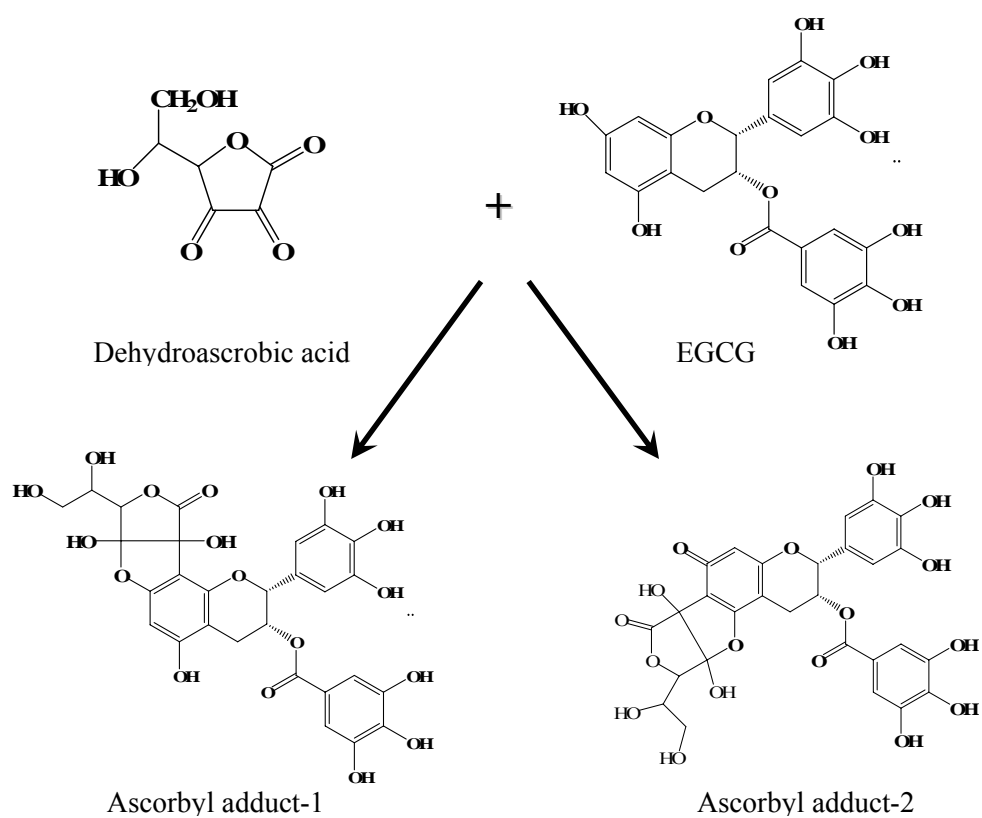


**Figure 9.** Formation of ascorbyl adducts from dehydroascorbic acid and EGCG

(Dr. Shengmin Sang's unpublished data)



## **Materials & Methods**

### **1. Development of derivatization and instrumentation methods for dicarbonyl compounds (MGO, GO) quantification**

#### **1.1 Derivatization method of MGO and GO**

As the derivative standards, Quinoxaline was purchased from Fluka and 2-methylquinoxaline was purchased from Aldrich. O-phenyldiamin (DB) was purchased from Sigma. MGO and GO were purchased from Fluka. To earn the reactant ratio and derivatization time of DB and MGO, the time course of the derivatization of MGO or GO (0.73 mmol) with DB (0.73 mmol, 3.65 mmol, 7.3 mmol, 14.6 mmol) was studied in phosphate buffer solution (50 mmol/L, pH 7.4) at 37 °C, respectively. The amount of methylquinoxaline or quinoxaline was monitored by analyzing aliquots (10 µL) of the incubation mixtures at different time points (0 min, 5 min, 10 min, 30 min, 60 min, 120 min and 240 min) during 4 h using the HPLC method detailed above.

#### **1.2 HPLC method for the quantifications of dicarbonyl compounds (MGO, GO)**

The level of methylquinoxaline and quinoxaline was analyzed using an HPLC system, consisting of a Waters 717 refrigerated autosampler, a Waters associates SP2A2 chromatography pump, and a UV-vis detector (Waters 490E programmable multiwavelength detector). A Supelcosil C<sub>18</sub> reversed-phase column (150 mm x 4.6 mm inner diameter; Supelco Co., Bellefonte, PA) was used. The HPLC was performed

under binary gradient elution, mobile phase A (95% acetonitrile and 5% water) and B (5% water and 95% acetonitrile) were used. All the solvents were filtered with 0.2  $\mu\text{m}$  Nylaflo Membrane filter and degassed. The flow rate was maintained at 1 mL/min, and the mobile phase began with 100% A. It was followed by progressive, linear increases in B to 40% at 35 min, 60% at 45 min, and 100% at 46 min. The mobile phase was then re-equilibrated to 100% at 52 min for 8 min. The injection volume was 50  $\mu\text{L}$  for each sample solution. The wavelength of UV detector was set at 280 nm for methylquinoxaline and 313 nm for quinoxaline. The limit of detection was  $\sim 100$  ng/mL and the limit of quantification was 1  $\mu\text{g/mL}$  for both methylquinoxaline and quinoxaline.

### 1.3 Calibration

Known amounts of EGCG, Methylquinoxaline, Quinoxaline were prepared in triplicate at seven different concentrations: EGCG (21.4 nM, 0.214  $\mu\text{M}$ , 2.14 $\mu\text{M}$ , 21.4 $\mu\text{M}$ , 0.214 mM, 2.14 mM, 21.4 mM); Methylquinoxaline (72.8 nM, 0.728 $\mu\text{M}$ , 7.28 $\mu\text{M}$ , 72.8 $\mu\text{M}$ , 0.728 mM, 7.28 mM, 72.8 mM); Quinoxaline (69.2 nM, 0.692 $\mu\text{M}$ , 6.92 $\mu\text{M}$ , 69.2 $\mu\text{M}$ , 0.692 mM, 6.92 mM, 69.2 mM). The HPLC analysis procedure was carried out as described above. Calibration curves were constructed by plotting the peak areas of EGCG, Methylquinoxaline, Quinoxaline against their concentrations.

### 1.4 Recovery

Recovery was obtained by comparing the Methylquinoxaline and Quinoxaline peak

areas obtained for the spiked samples with those obtained from nonspiked samples in which equivalent amounts of synthetic Methylquinoxaline and Quinoxaline have been added following derivatization and procedure described in a quantification method.

## **2. Reaction conditions of EGCG and MGO *in vitro* model**

### **2.1 Reactant ratio of the EGCG and MGO**

Sodium Phosphate buffer (50 mmol/L, pH 7.4) was employed as the reaction medium to mimic the physical condition. An aliquot (10 mg, 0.022 mmol) of EGCG was dissolved in 1.5 mL buffer solution. The molar ratio of EGCG to MGO was set up as 6:1; 3:1; 2:1; 1:1; 1:2; 1:3; and 1:6. MGO (0.0037 mmol; 0.0073 mmol; 0.011 mmol; 0.022 mmol; 0.044 mmol; 0.066 mmol; 0.132 mmol) were mixed with EGCG solutions, respectively. The mixtures were incubated in 37 ° C water bath for 60 min. Then 10 µL samples was diluted and subjected to HPLC analysis for each reaction.

### **2.2 Incubation time course study of EGCG and MGO**

To obtain the reaction time of EGCG and MGO, the amounts of EGCG and MGO were monitored by HPLC in the 2 hours' reaction. An aliquot (10 mg, 0.022 mmol) EGCG was dissolved in 1.5 mL buffer solution (50 mmol/L, pH 7.4). After the addition of MGO (1.31 mg, .0.0073 mmol), the mixture was incubated in 37 ° C water bath. Then 50µl mixed solution was picked out at different time points (5 min, 10 min, 15 min, 20 min, 30 min, 40 min, 60 min and 120 min). Acetic acid (1 µL) was added for the inhibition of the reaction between EGCG and MGO. 100 µL DB-ethanol

solutions ( $2.43 \times 10^{-4}$  mol/L) were prepared with the mixture for the derivatization. After the incubation in 37 °C water bath for another 40 min, 10 µL samples were diluted 10 times for further HPLC analysis.

### **3. Developing effective method to inhibit the reaction between EGCG and MGO**

Acetic acid and Ascorbic Acid was separately used for the pH adjustment. Four phosphate buffer solutions (50 mmol/L) with different pH were prepared (pH 3.0, 4.0, 5.0, 7.4). An aliquot (10 mg, 0.022 mmol) EGCG was dissolved in 1.5 mL those four buffer solutions, separately. After adding MGO (1.31 mg, .0.0073 mmol), the mixture solution was incubated in 37 °C water bath. Then 10µl mixture solution was picked out at different time points (5 min, 10 min, 15 min, 20 min, 30 min, and 40 min). 100 µL DB-ethanol solutions ( $2.43 \times 10^{-4}$  mol/L) were added to the mixture solution for the derivatization. The mixture solution was incubated in 37 °C water bath for another 40 min and prepared for HPLC analysis.

### **4. Trapping effect of dicarbonyl compounds by EGCG**

Trapping effect was measured base on the decreasing level of MGO in a 60 min incubation process with EGCG. MGO (2.0 mM) or GO (2.0 mM) was incubated with 6 mM EGCG in pH 7.4 phosphate buffer solutions at 37°C and shaken at 40 rpm speed for 5, 10, 15, 20, 30, 40, and 60 min. Then the triplicated vials at each time point were added 1µL acetic acid to stop the reaction and 100 mM DB to derivatize the remaining MGO or GO using method detailed above.

### **5. LC/ESI-MS analysis of EGCG and its MGO or GO adducts.**

LC/MS analysis was carried out with a Finnigan Spectra System which consisted of a Surveyor MS pump plus, a Surveyor refrigerated autosampler plus, and a LTQ linear ion trap mass detector (ThermoFinnigan, San Jose, CA) incorporated with electrospray ionization (ESI) interface. A  $50 \times 2.0$  mm i.d., 3  $\mu$ m Gemini C<sub>18</sub> column (Phenomenex) was used for separation with a flow rate of 0.2 mL/min. The column elution started with 3-min isocratic phase of 100% solvent A (5% aqueous methanol with 0.2% acetic acid), followed by progressive, linear increases in B (95% aqueous methanol with 0.2% acetic acid) to 20% at 33 min and 100% at 45 min for 5 min. The mobile phase was then re-equilibrated to 100% A at 51 min for 10 min. The LC elute was introduced into the ESI interface. The negative ion polarity mode was set for ESI ion source with the voltage on the ESI interface maintained at approximately 5 kV. Nitrogen gas was used as the sheath gas at a flow rate of 30 arb units and the auxiliary gas at 5 arb units, respectively. The structural information of EGCG and the major MGO or GO adducts was obtained by tandem mass spectrometry (MS/MS) through collision-induced dissociation (CID) with a relative collision energy setting of 30%.

### **6. Studying the formation of MGO or GO adducts of EGCG using LC/MS.**

EGCG (14.6 mM) was incubated with different concentrations of MGO or GO (4.87, 14.6, and 43.8 mM) in pH 7.4 phosphate buffer solutions at 37°C for 60 min, respectively. Then 10  $\mu$ L samples were taken and transferred to vials containing 190  $\mu$ L of a solution containing 0.2% ascorbic acid and 0.05% EDTA to stabilize EGCG and

the MGO or GO adducts of EGCG. These samples were immediately analyzed or stored at -80 °C before analyzing by LC/MS.

#### 7. Purification of the major mono-MGO adducts of EGCG

EGCG (1.0 g, 2.2 mmol) and MGO (0.131g, 0.73mmol) were dissolved in 150 mL phosphate buffer (50mmol/L, pH 7.4) and then kept at 37 ° C for 60 min. After extraction with ethyl acetate and evaporating the solvent *in vacuo*, the residue was loaded to Sephadex LH-20 column eluted with ethanol to remove the remaining EGCG, and then to RP C-18 column eluted with 20% methanol aqueous to obtain EGCGMGO-1 (51.2 mg) and EGCGMGO-2 (45.8 mg). <sup>1</sup>H and <sup>13</sup>C NMR data of EGCGMGO-1 and EGCGMGO-2 were listed in Table 1, and negative ESI-MS of both compounds were m/z 529 [M-H]<sup>-</sup>.

#### 8. NMR.

<sup>1</sup>H (400 MHz), <sup>13</sup>C (100 MHz), and all 2D NMR spectra were acquired on a Varian 400 instrument (Varian Inc., Palo Alto, CA). Compounds were analyzed in CD<sub>3</sub>OD, with TMS as internal standard. <sup>1</sup>H-<sup>13</sup>C HMQC (heteronuclear multiple quantum correlation) and HMBC (heteronuclear multiple band correlation) experiments were performed as described previously (Fang *et al.*, 2001).

## Results

### 1. Derivatization of MGO and GO with 1,2-diaminobenzene (DB).

The best current assay to determine the levels of MGO and GO involve derivatization of MGO and GO with 1,2-diaminobenzene (DB) and its derivatives, followed by quantification of the resulting quinoxalines by HPLC with ultraviolet, spectrophotometric, fluorescence, or mass detection (*Espinosa-Mansilla et al., 1998; Akira et al., 1994; Odani et al., 1999; Nemet et al., 2004*). In our study, we developed our own HPLC-UV method by modification of existing methods to quantify MGO and GO using DB as derivatization agent (Figure 11). The effects of reaction time, pH of reaction medium, and the concentration of DB on the formation of quinoxalines were studied. Our data shown that DB could effectively react with MGO and GO within 10 min and 10-20 fold of DB were sufficient for the derivatization (Figures 12 and 13). In addition, we found that the pH of the reaction medium did not influence the derivatization (Figure 14).

### 2. Trapping of MGO and GO by EGCG under physiological conditions.

In our studies, we found that EGCG could efficiently trap MGO and GO under physiological conditions (pH 7.4, 37 °C). More than 90% MGO was trapped within 5 min and 70% GO was trapped within 1 hour (Figure 15). In this study, we quantified the levels of MGO and GO using an HPLC-UV method after derivatization by DB to form methylquinoxaline and quinoxaline, respectively. In addition, we found that

EGCG could not trap reactive dicarbonyl compounds under acid conditions ( $\text{pH} < 4$ ) (Figure 16).

### 3. Studying the formation of MGO or GO adducts of EGCG using LC/MS.

In order to understand the mechanism by which EGCG traps MGO or GO, we studied the formation of carbonyl adducts under different ratio between EGCG and MGO or GO (3:1, 1:1, and 1:3) using LC/MS (Figures 17 and 18). In 3:1 ratio, we found mono-MGO or mono-GO adducts were the major products. During the incubation of EGCG and MGO (3:1), three major new peaks appeared in the LC spectra (Figure 10). They all had the same molecular ion ( $529 [\text{M}-\text{H}]^-$ ) and MS/MS fragments, but different retention times. All three compounds had the fragment ( $457 [\text{M}-72-\text{H}]^-$ ) that lost one MGO ( $m/z$ : 72) molecule (Figure 10) indicating they were mono-MGO adducts of EGCG and the fragments ( $359 [\text{M}-170-\text{H}]^-$  and  $377 [\text{M}-152-\text{H}]^-$ ) that exhibited the typical loss of one gallic acid group ( $\text{M}-170$ ) and one galloyl group ( $\text{M}-152$ ) indicating the conjugation did not occur on the gallate ring of EGCG. There were four major new peaks appeared in the LC spectra after incubation of EGCG and GO (3:1) (Figure 20). They all had the same molecular ion ( $515 [\text{M}-\text{H}]^-$ ) and MS/MS fragments, but different retention times. All four compounds had the fragment ( $457 [\text{M}-72-\text{H}]^-$ ) that lost one GO ( $m/z$ : 58) molecule (Figure 13) indicating they were mono-GO adducts of EGCG and the fragments ( $345 [\text{M}-170-\text{H}]^-$  and  $363 [\text{M}-152-\text{H}]^-$ ) that exhibited the typical loss of one gallic acid group ( $\text{M}-170$ ) and one galloyl group ( $\text{M}-152$ ) indicating the conjugation did not occur on the gallate ring of EGCG.



In 1:1 ratio, the amount of mono-MGO adducts and mono-GO adducts increased in comparison to 3:1 ratio, and di-MGO adducts and di-GO adducts were formed as minor products (Figures 17 and 18). In 1:3 ratio, we found Di-MGO adducts and mono- and di-GO adducts were the major products after incubation EGCG with MGO and GO, respectively (Figures 17 and 18). During the incubation of EGCG and MGO (1:3), five major new peaks appeared in the LC spectra (Figures 17 and 21). They all had the same molecular ion ( $601 [M-H]^-$ ) and MS/MS fragments, but different retention times. All five compounds had the fragment ( $529 [M - 72-H]^-$ ) that lost one MGO ( $m/z$ : 72) molecule (Figure 21). This fragment had almost identical MS/MS fragments as those from mono-MGO adduct of EGCG. All of these features indicated that they were di-MGO adducts of EGCG. In addition, all of these compounds had the fragments ( $431 [M - 170-H]^-$  and  $449 [M - 152-H]^-$ ) that exhibited the typical loss of one gallic acid group (M-170) and one galloyl group (M-152) indicating the conjugation did not occur on the gallate ring of EGCG. There were four major new peaks appeared in the LC spectra after incubation of EGCG and GO (1:3) (Figures 18 and 22). Two of them had the same molecular ion ( $515 [M-H]^-$ ), MS/MS fragments, and retention times as those observed from the 3:1 ratio, respectively. The other two peaks had the molecular ion  $573 [M - H]^-$ , which were 116 ( $58 \times 2$ ) mass units higher than that of EGCG indicating they were di-GO adducts of EGCG. Both of them had the fragments ( $403 [M - 170-H]^-$  and  $421 [M - 152-H]^-$ ) that exhibited the typical loss of one gallic acid group (M-170) and one galloyl group (M-152) indicating the conjugation did not occur on the gallate ring of EGCG.

#### 4. Purification and structure elucidation of the major mono-MGO adducts of EGCG

We have purified the acetylated derivatives of two mono-MGO adducts of EGCG using chiral column and determined their structures after analyzing the NMR data of the acetylated derivatives (*Lo et al., 2006*). In this study, we have successfully purified two major mono-MGO adducts of EGCG, EGCGMGO-1 and EGCGMGO-2, without derivatization (Figure 23).

EGCGMGO-1 was assigned the molecular formula  $C_{25}H_{22}O_{13}$  based on negative-ion ESI-MS ( $[M-H]^-$  at  $m/z$  529) and  $^{13}C$  NMR data. Its  $^1H$ - and  $^{13}C$ - NMR spectra showed very similar patterns as those of EGCG (Table 1). The  $^1H$ -NMR spectrum of EGCGMGO-1 exhibits signals for B ring (H-2', 6' at  $\delta_H$  6.51 s), C ring (H-2 at  $\delta_H$  5.02 s, H-3 at  $\delta_H$  5.53 m, and H-4 at  $\delta_H$  2.99 dd 4.0, 17.2 and 2.88 brd 17.2), and D ring (H-2'', 6'' at  $\delta_H$  6.91 s) (Figure 24), which were similar to those of EGCG, indicating that the B, C, and D rings of EGCGMGO-1 do not undergo any changes. In comparison with the  $^1H$ -NMR spectrum of EGCG, EGCGMGO-1 only showed one singlet signal for one proton of A ring ( $\delta_H$  6.06 s), instead of the one singlet signal for two protons of EGCG ( $\delta_H$  5.96 s 2H), and two additional proton signals for MGO group ( $\delta_H$  5.61 s, 1H and 2.13 s, 3H). The major differences in the  $^{13}C$  spectra of EGCGMGO-1 (Figure 16) and EGCG were (a) the presence of three additional carbons at  $\delta_C$  25.6 t, 72.7 d, and 211.0 s for MGO group in EGCGMGO-1; and (b) the quaternary carbon observed at  $\delta_C$  105.3 in lieu of an unsubstituted aromatic carbon

from the A ring of EGCG. In addition, the molecular weight of EGCGMGO-1 was 72 (M.W. of MGO: 72) mass units higher than that of EGCG. All of these spectral features supported the presence of a MGO group in EGCGMGO-1, which was located at C-8 or C-6 position of A ring. The HMBC spectrum showed correlations between  $\delta_C$  154.8 and H-2 ( $\delta_H$  5.02 ppm),  $\delta_C$  154.8 and H-4 ( $\delta_H$  2.99 and 2.88 ppm), and  $\delta_C$  158.3 and H-4, thus establishing the signal at  $\delta_C$  154.8 ppm as that of C-9 and  $\delta_C$  158.3 ppm as that of C-5 (Figures 26 and 27). This carbon nucleus resonating at  $\delta_C$  154.8 ppm showed no coupling to the only A-ring proton ( $\delta$  6.06 ppm), whereas the carbon at  $\delta_C$  158.3 ppm had a cross peak with the only A-ring proton in the HMBC spectrum. Therefore, the MGO group was located at the C-8 position of A-ring. This was further confirmed by the cross peaks in the HMBC spectrum (Figure 11) between  $\delta_C$  154.8 (C-9) and H-11 ( $\delta_H$  5.61 s),  $\delta_C$  105.3 (C-8) and H-11 ( $\delta_H$  5.61 s). Thus, the structure of EGCGMGO-1 was identified as shown in Figure 10.

The negative-ion ESI-MS of EGCGMGO-2 displayed a molecular ion peak at  $m/z$  [M-H]<sup>-</sup> 529, supporting a molecular formula of C<sub>25</sub>H<sub>22</sub>O<sub>13</sub>, which was the same as that of EGCGMGO-1. The NMR spectra of EGCGMGO-2 showed signal patterns similar to those of EGCGMGO-1 (Tables 1). The <sup>1</sup>H NMR spectrum of EGCGMGO-2 displayed signals for B ring (H-2', 6' at  $\delta_H$  6.47 s), C ring (H-2 at  $\delta_H$  5.05 s, H-3 at  $\delta_H$  5.51 m, and H-4 at  $\delta_H$  2.99 dd 4.0, 17.2 and 2.88 brd 17.2), and D ring (H-2'', 6'' at  $\delta_H$  6.92 s), only one proton (singlet signal) for A ring ( $\delta_H$  6.06 s), and two additional proton signals for MGO group ( $\delta_H$  5.56 s, 1H and 2.15 s, 3H) (Figure 29). The

$^{13}\text{C}$ -NMR spectrum of EGCGMGO-2 displayed 25 carbon signals, 15 of which were assigned to the A, B and C ring of flavan-3-ols, 7 of which were the signals for the gallate group and three were for the MGO group ( $\delta_{\text{C}}$  25.9 t, 72.6 d, and 212.1 s) (Table 1 and Figure 30). Similarly, one quaternary carbon and one unsubstituted aromatic carbon were observed at  $\delta_{\text{C}}$  105.5 and 96.3 ppm instead of two unsubstituted aromatic carbon from the A ring. These spectra indicated the presence of a MGO group also located at A ring in EGCGMGO-2. The HMBC spectrum showed correlations between  $\delta_{\text{C}}$  155.1 and H-2 ( $\delta_{\text{H}}$  5.05 ppm),  $\delta_{\text{C}}$  155.1 and H-4 ( $\delta_{\text{H}}$  2.99 and 2.88 ppm), and  $\delta_{\text{C}}$  158.3 and H-4, thus establishing the signal at  $\delta_{\text{C}}$  155.1 ppm as that of C-9 and  $\delta_{\text{C}}$  158.3 ppm as that of C-5 (Figures 27 and 31). This carbon nucleus resonating at  $\delta_{\text{C}}$  155.1 ppm showed no coupling to the only A-ring proton ( $\delta$  6.06 ppm), whereas the carbon at  $\delta_{\text{C}}$  158.3 ppm had a cross peak with the only A-ring proton in the HMBC spectrum. Therefore, the MGO group was also located at the C-8 position of A ring. This was further confirmed by the cross peaks in the HMBC spectrum (Figure 31) between  $\delta_{\text{C}}$  155.1 (C-9) and H-11 ( $\delta_{\text{H}}$  5.61 s),  $\delta_{\text{C}}$  105.3 (C-8) and H-11 ( $\delta_{\text{H}}$  5.61 s). Therefore, the difference between EGCGMGO-1 and EGCGMGO-2 was the stereochemistry of the newly formed hydroxyl group at position 11, one has the R-configuration and the other had the S-configuration. Full assignments of the  $^1\text{H}$  and  $^{13}\text{C}$  NMR signals of EGCGMGO-1 and EGCGMGO-2 were made by analyzing the signals in HMBC and HMQC spectra (Table 1 and Figures 26, 28, 31, and 32).

**Table 1.**  $\delta_{\text{H}}$  (400 MHz) and  $\delta_{\text{C}}$  (100 MHz) NMR spectra data of **EGCGMGO-1** and **EGCGMGO-2** ( $\text{CD}_3\text{OD}$ ) ( $\delta$  in ppm)

Position	<b>EGCGMGO-1</b>		<b>EGCGMGO-2</b>	
	$\delta_{\text{H}}$	$\delta_{\text{C}}$	$\delta_{\text{H}}$	$\delta_{\text{C}}$
2	5.02 s	78.9 d	5.05 s	79.1 d
3	5.53 m	69.6 d	5.51 m	69.6 d
4	2.99 dd 4.0, 17.2 2.88 brd 17.2	27.0 t	2.99 dd 4.0, 17.2 2.88 brd 17.2	26.9 t
5		158.3 s		158.3 s
6	6.06 s	96.4 d	6.06 s	96.3 d
7		156.9 s		156.7 s
8		105.3 s		105.5 s
9		154.8 s		155.1 s
10		99.6 s		99.6 s
11	5.61 s	72.7 d	5.56 s	72.6 d
12		211.0 s		212.1 s
13	2.13 s	25.6 t	2.15 s	25.9 t
1'		130.3 s		130.3 s
2'	6.51 s	106.6 d	6.47 s	106.8 d
3'		146.6 s		146.6 s
4'		133.7 s		133.8 s
5'		146.6 s		146.6 s
6'	6.51 s	106.6 d	6.47 s	106.8 d
1''		121.4 s		121.4 s
2''	6.91 s	110.2 d	6.92 s	110.2 d
3''		146.2 s		146.3 s
4''		139.7 s		139.7 s
5''		146.2 s		146.3 s
6''	6.91 s	110.2 d	6.92 s	110.2 d
7''		167.5 s		167.6 s

## Discussion

Many studies have shown that dietary flavonoids, which are widely distributed in fruits, vegetables, grains, and beverages, such as tea, coffee, and wine, are strong antioxidants and may prevent diabetes and its complications. However, it is unclear that through what mechanisms dietary flavonoids prevent the development of diabetic complications. Carbonyl stress is an important mechanism of tissue deterioration in several pathological conditions, such as diabetes complications, Alzheimer's disease, and general aging. Previous studies have demonstrated that reactive dicarbonyl compounds irreversibly and progressively modified proteins over time and yielded advanced glycation end products (AGEs), which are thought to contribute to the development of diabetes mellitus and its complications. Higher levels of  $\alpha$ -dicarbonyl compounds (e.g., MGO and GO) were observed in diabetic patients' plasma than those in healthy people's plasma (by 2-6 fold). Thus decreasing the levels of MGO and GO will be an effective approach to reduce the formation of AGEs and the development of diabetic complications. Several pharmaceutical agents have been shown to inhibit the formation of AGEs by trapping reactive dicarbonyl compounds. The application of these pharmaceutical agents was limited due to their side effects. Therefore, if non-toxic dietary compounds can be developed into a preventive agent for diabetic complications, the public health benefit would be tremendous. In this study, we found that EGCG, the major bioactive green tea polyphenol, could efficiently trap reactive dicarbonyl compounds (MGO and GO) to form mono- and di-

MGO or GO adducts under physiological conditions (pH 7.4, 37 °C). Our LC/MS and NMR data showed that positions 6 and 8 of the EGCG A ring were the major active sites for trapping reactive dicarbonyl compounds. We also found that EGCG could not trap reactive dicarbonyl compounds under acid conditions (pH < 4) indicating that slight base conditions can facilitate the trapping effects of EGCG. The trapping effect of GO is much slower comparing to MGO by EGCG in our study (**Figure 15**). Previous studies indicated that the hydrated monomer is the main form of glyoxal in aqueous solution. However, this hydrated monomer tends to polymerize to glyoxal dimer and trimer. The equilibrium between monomer and dimer and trimer has a very small constant value. So, the trapping reaction between EGCG and dicarbonyl form glyoxal was slowed by the transform from trimer or dimer glyoxal to dicarbonyl monomer glyoxal (*EUROPEAN COMMISSION, 2005*). Whether EGCG can trap reactive dicarbonyl species in vivo and thus reduce the formation of AGEs and prevent the development of diabetic complications need to be further studied. The purified mono-MGO adducts of EGCG in this study can be used as standards for further in vivo study.

**Figure 10. Sample preparation, incubation conditions, and derivatization procedure**

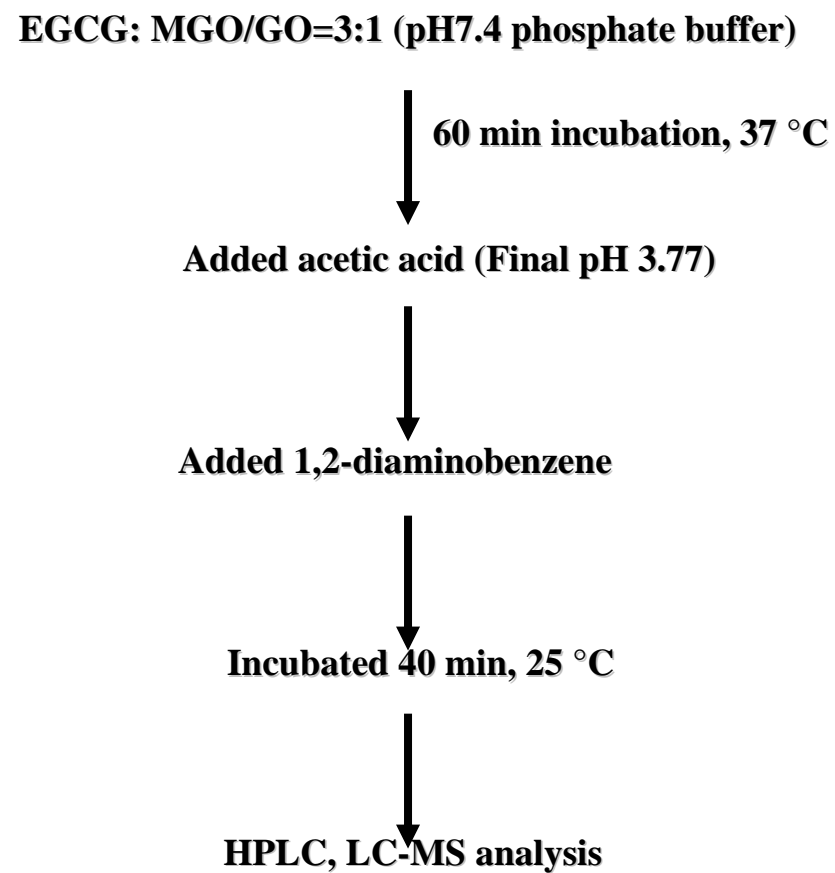
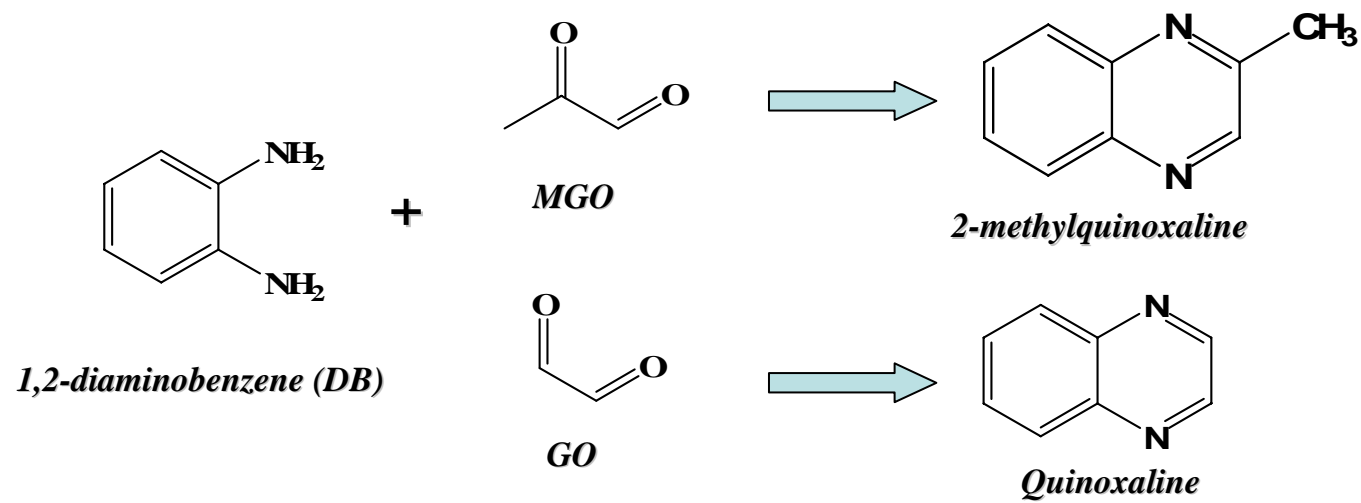




Figure 11. Formation of Methylquinoxaline and Quinoxaline



**Figure 12.** Time course of the derivatization of MGO with 1,2-diaminobenzene (DB) under physiological conditions (37°C, pH 7.4)

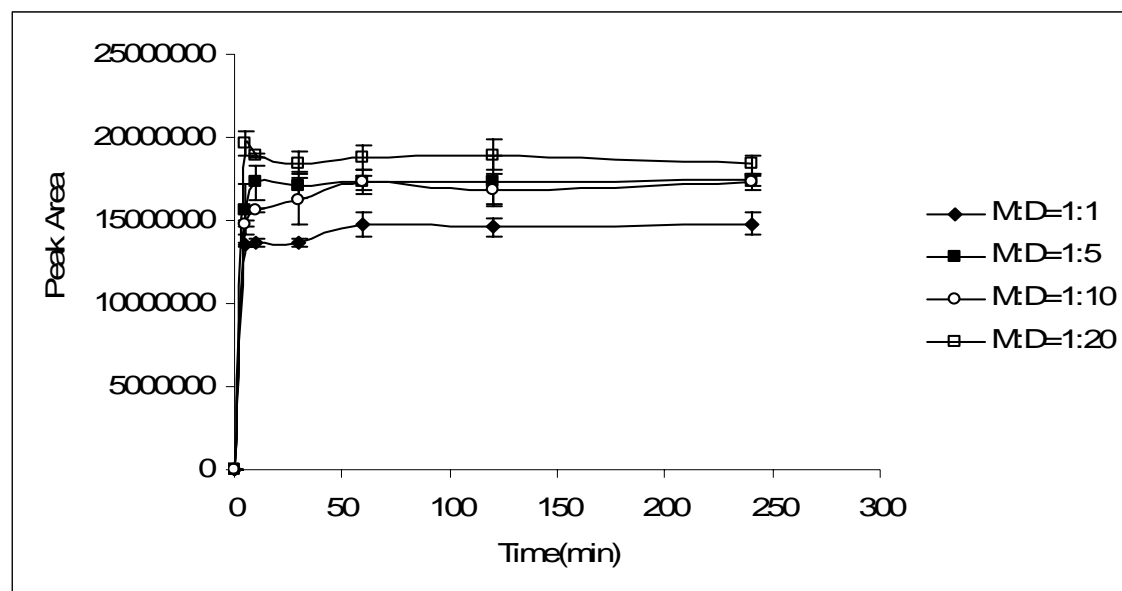
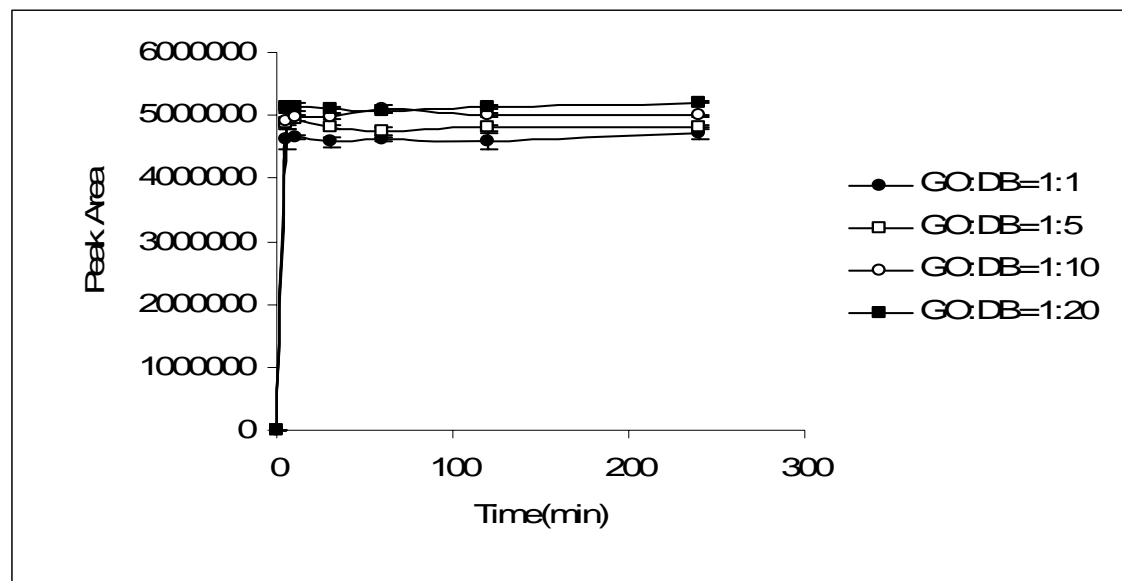
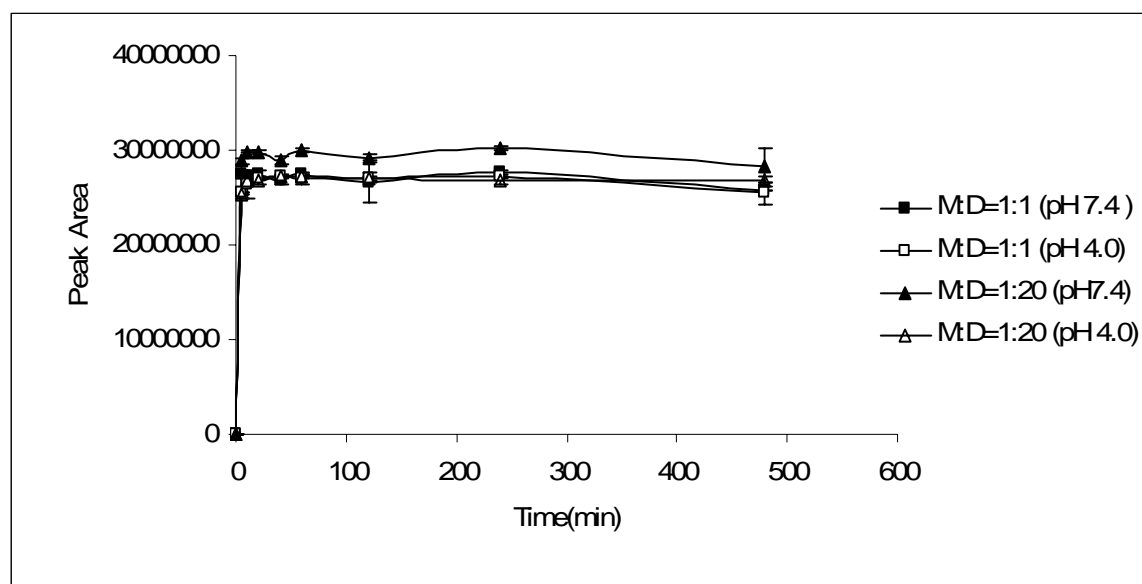


Figure 13. Time course of the derivatization of GO with 1,2-diaminobenzene (DB) under physiological conditions (37°C, pH 7.4)



**Figure 14.** The effect of pH on derivatization of MGO with 1,2-diaminobenzene (DB) at 37°C



**Figure 15. Trapping of MGO and GO by EGCG under physiological conditions (37 °C, pH 7.4)**

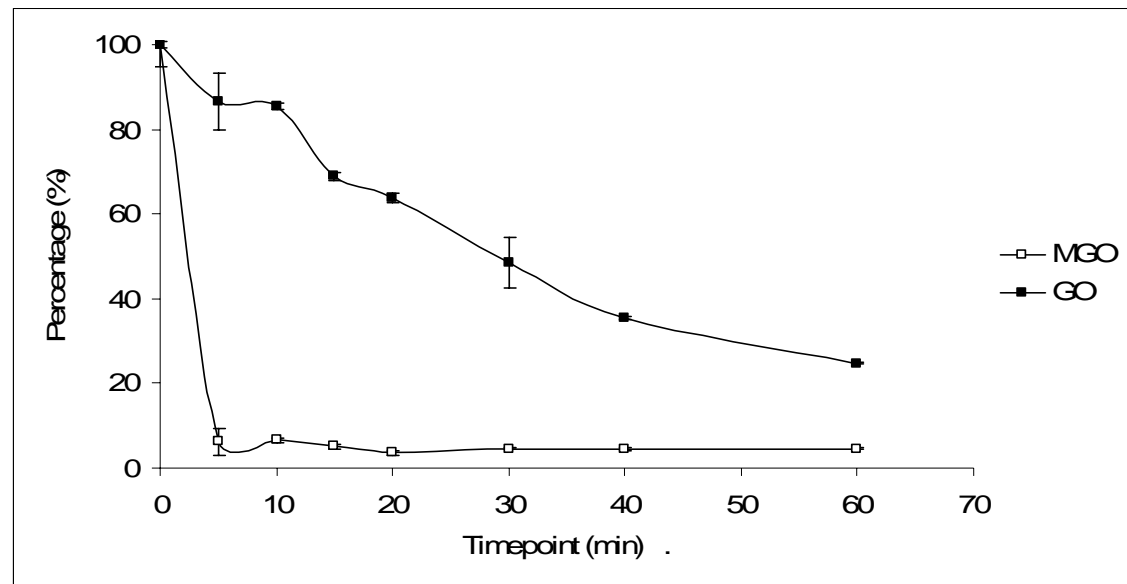


**Figure 16.** The effect of pH on the trapping of MGO by EGCG at 37°C

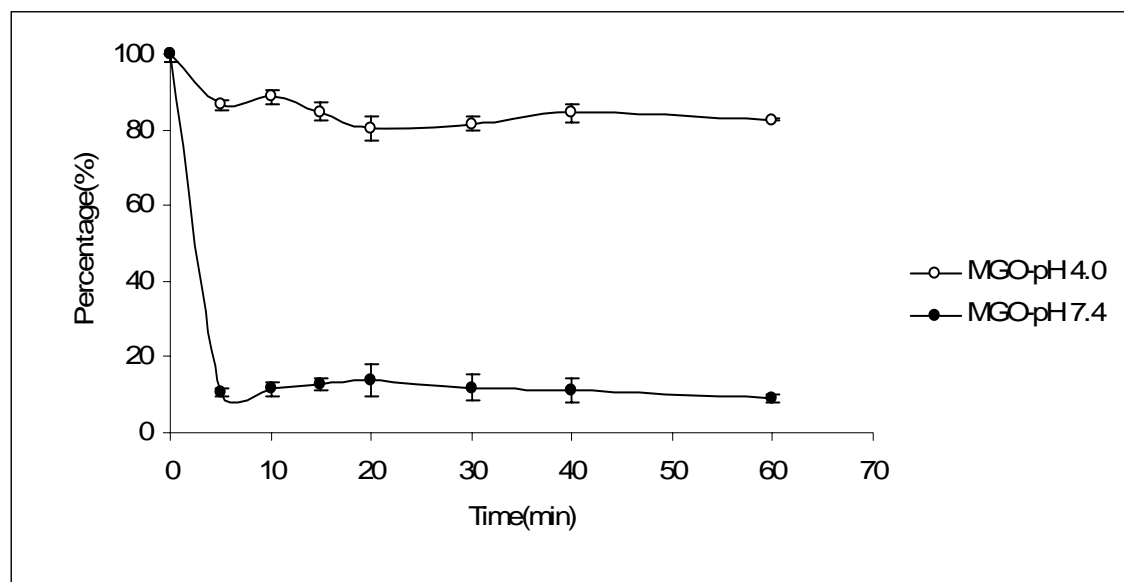


Figure 17. LC total ion chromatogram of EGCG after incubation of different ratio of MGO (3:1, 1:1, and 1:3) for 60 min

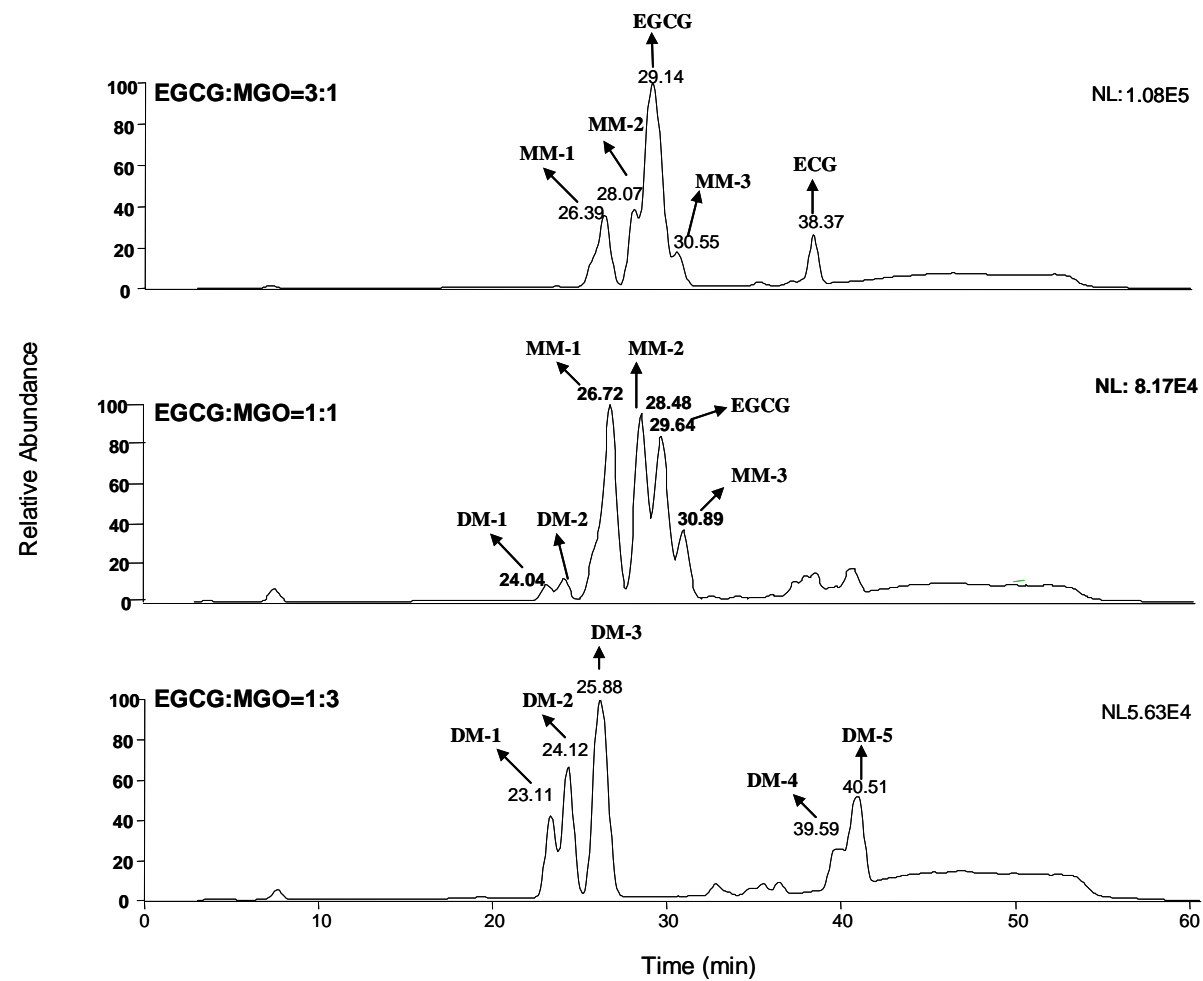
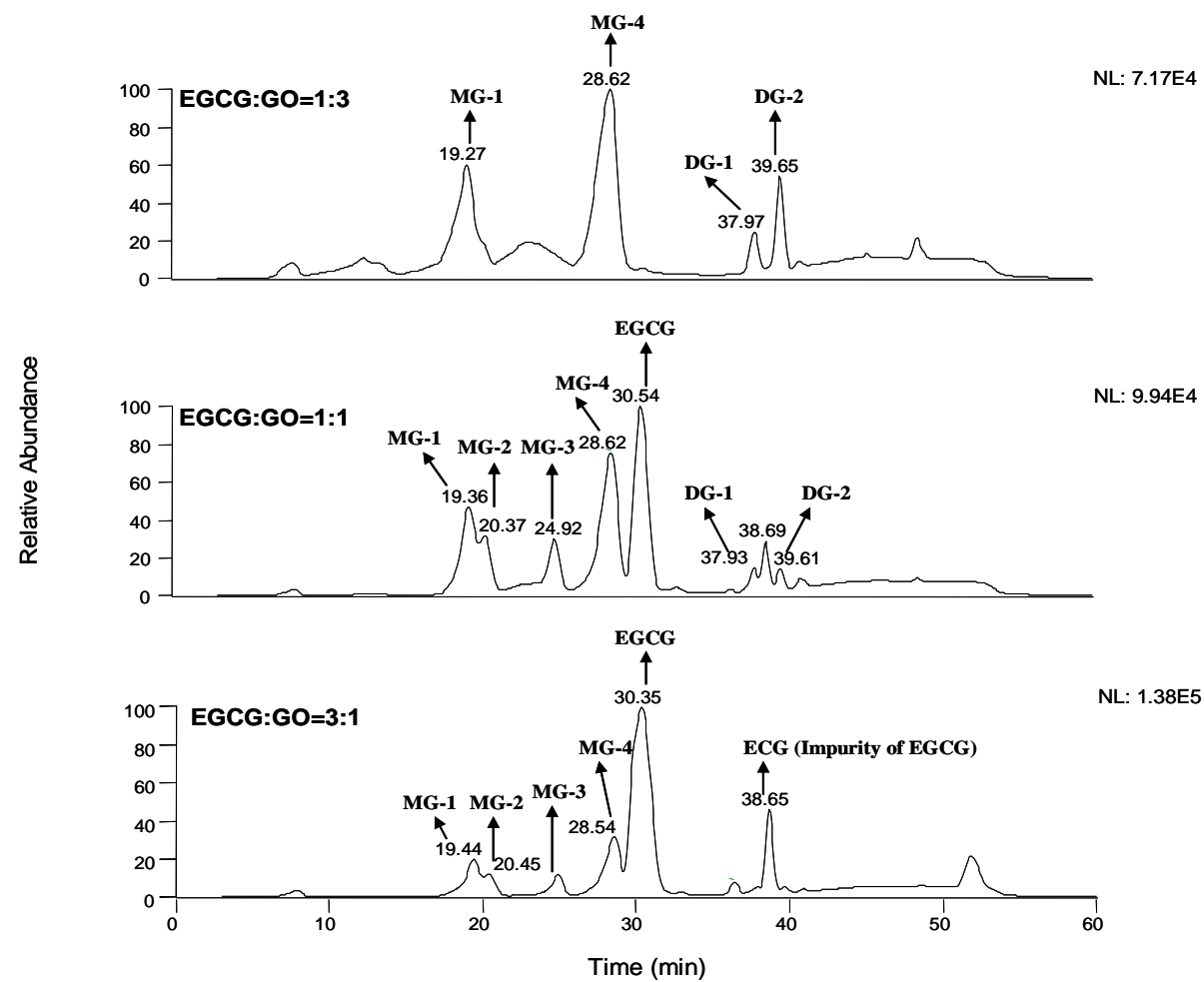


Figure 18. LC total ion chromatogram of EGCG after incubation of different ratio of GO (3:1, 1:1, and 1:3) for 60 min





**Figure 19. LC/MS/MS spectra of mono-MGO adducts of EGCG**

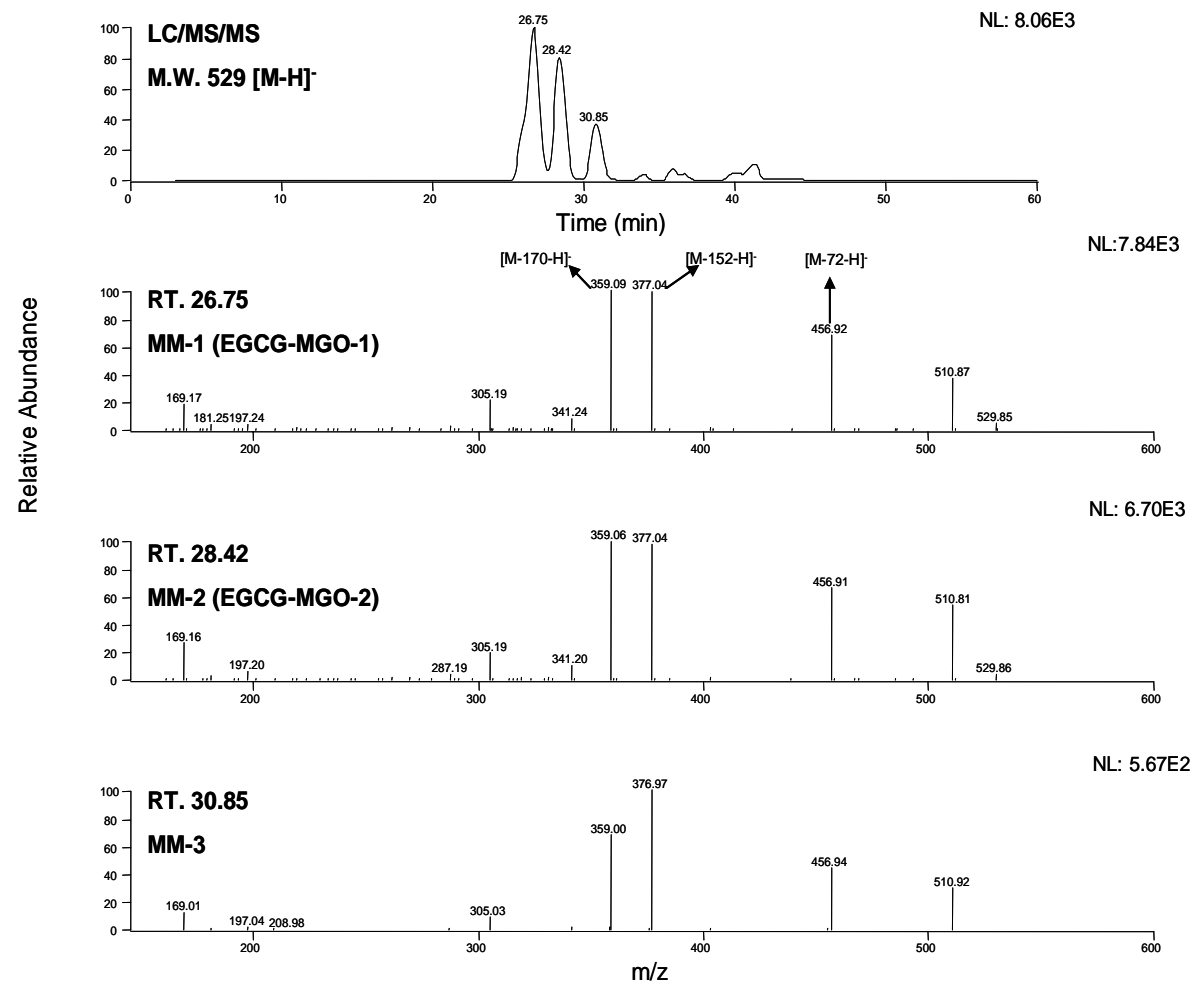


Figure 20. LC/MS/MS spectra of mono-GO adducts of EGCG

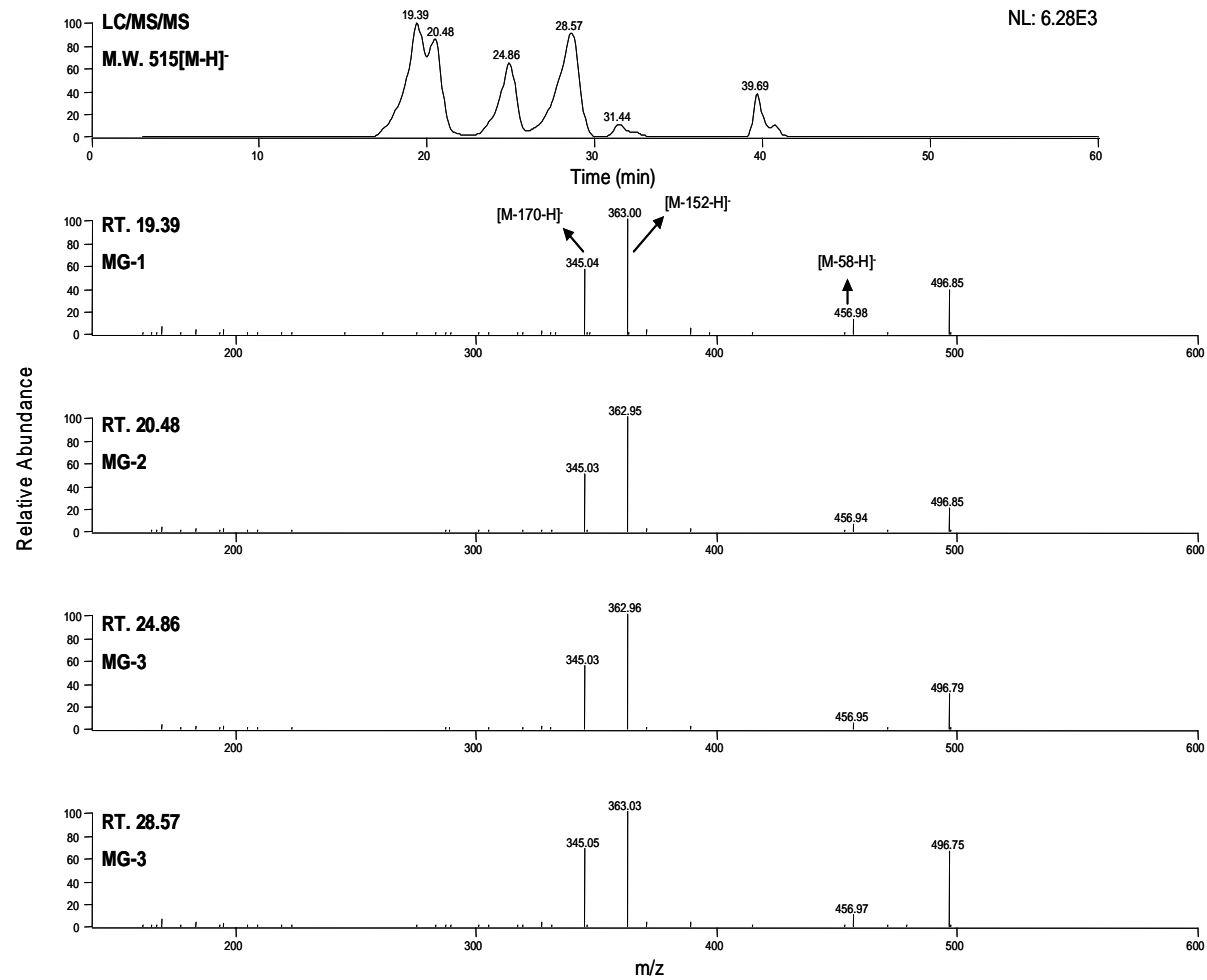


Figure 21. LC/MS/MS spectra of di-MGO adducts of EGCG

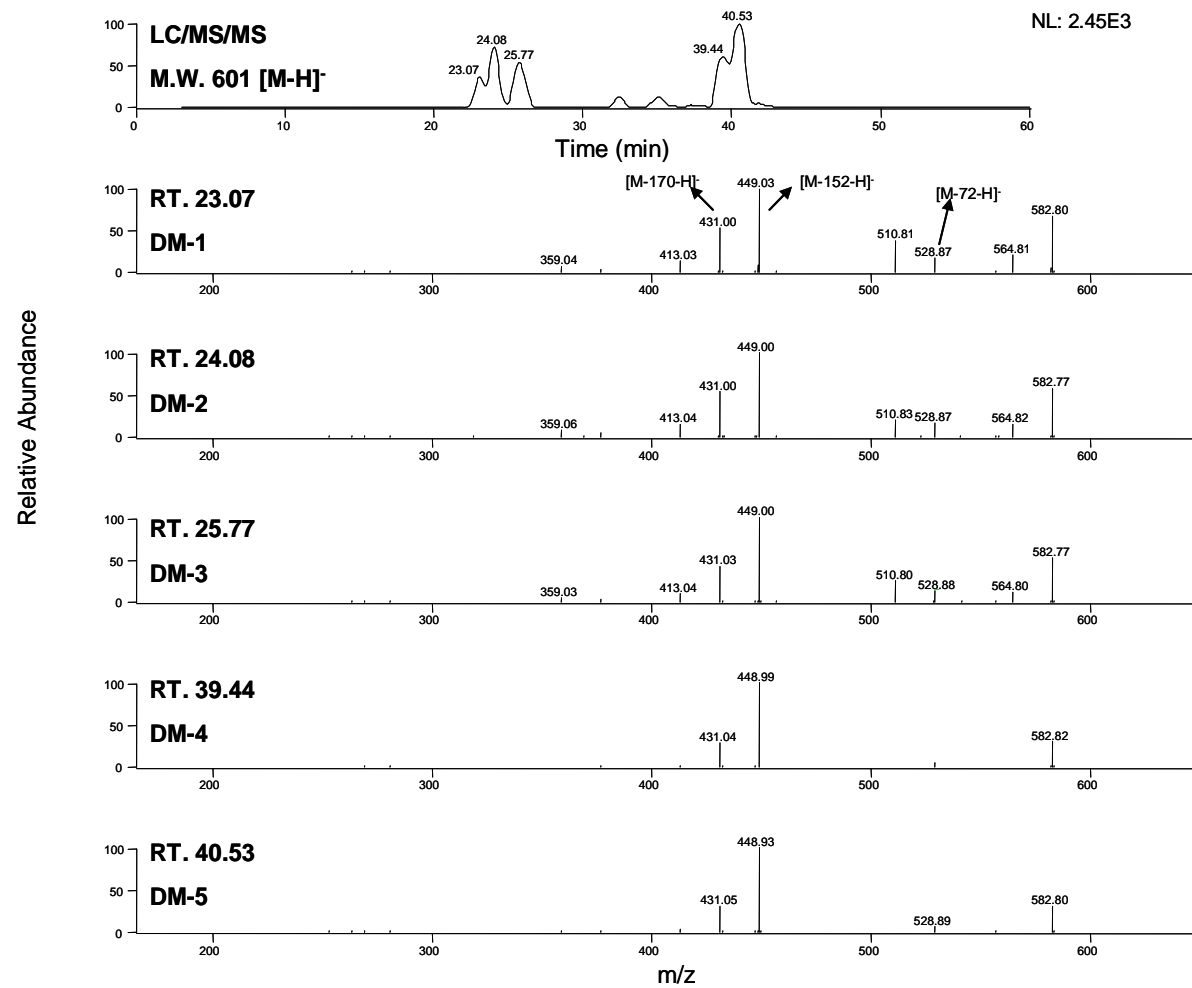
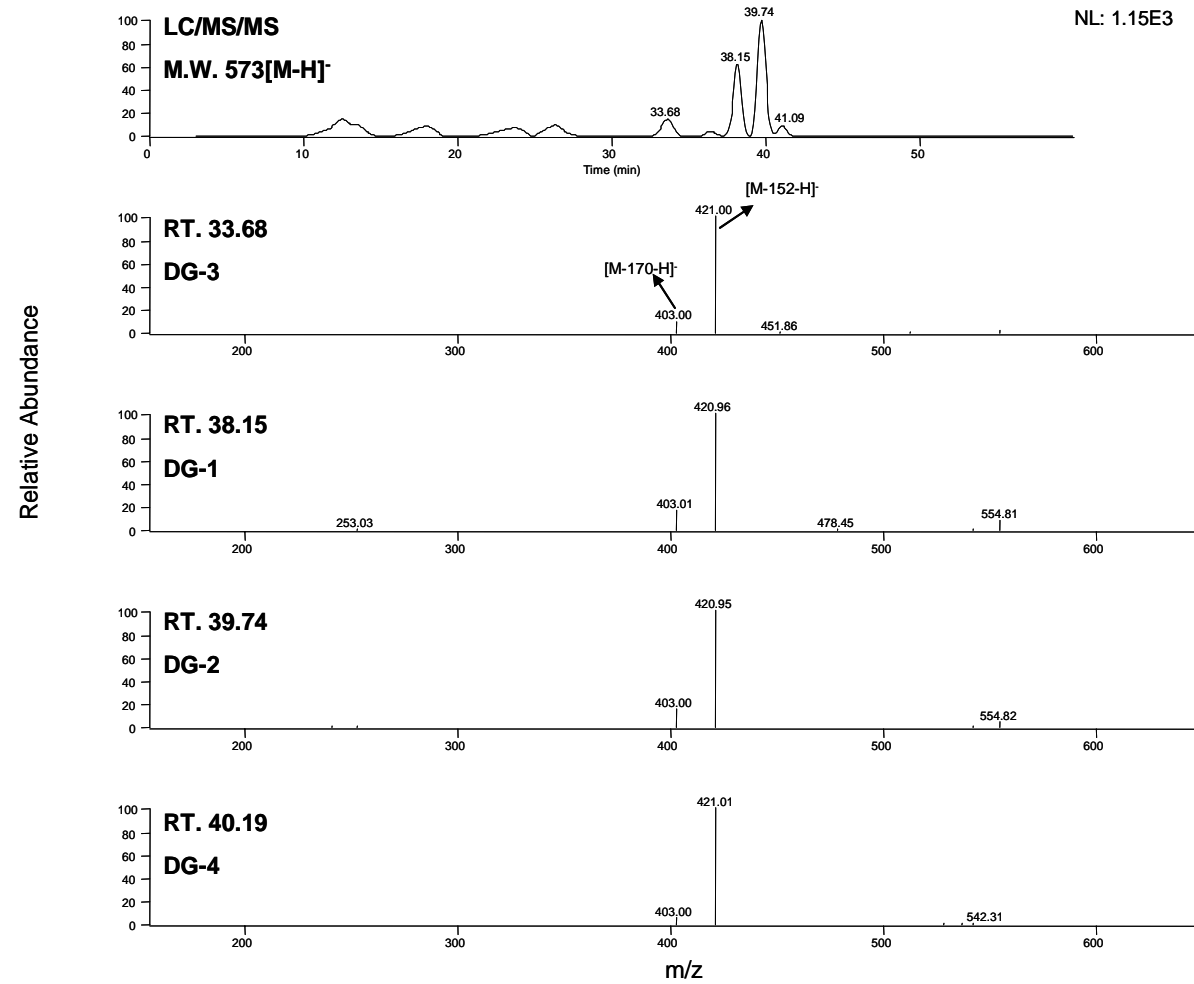


Figure 22. LC/MS/MS spectra of di-GO adducts of EGCG



**Figure 23. Formation of the Mono-MGO adducts of EGCG**

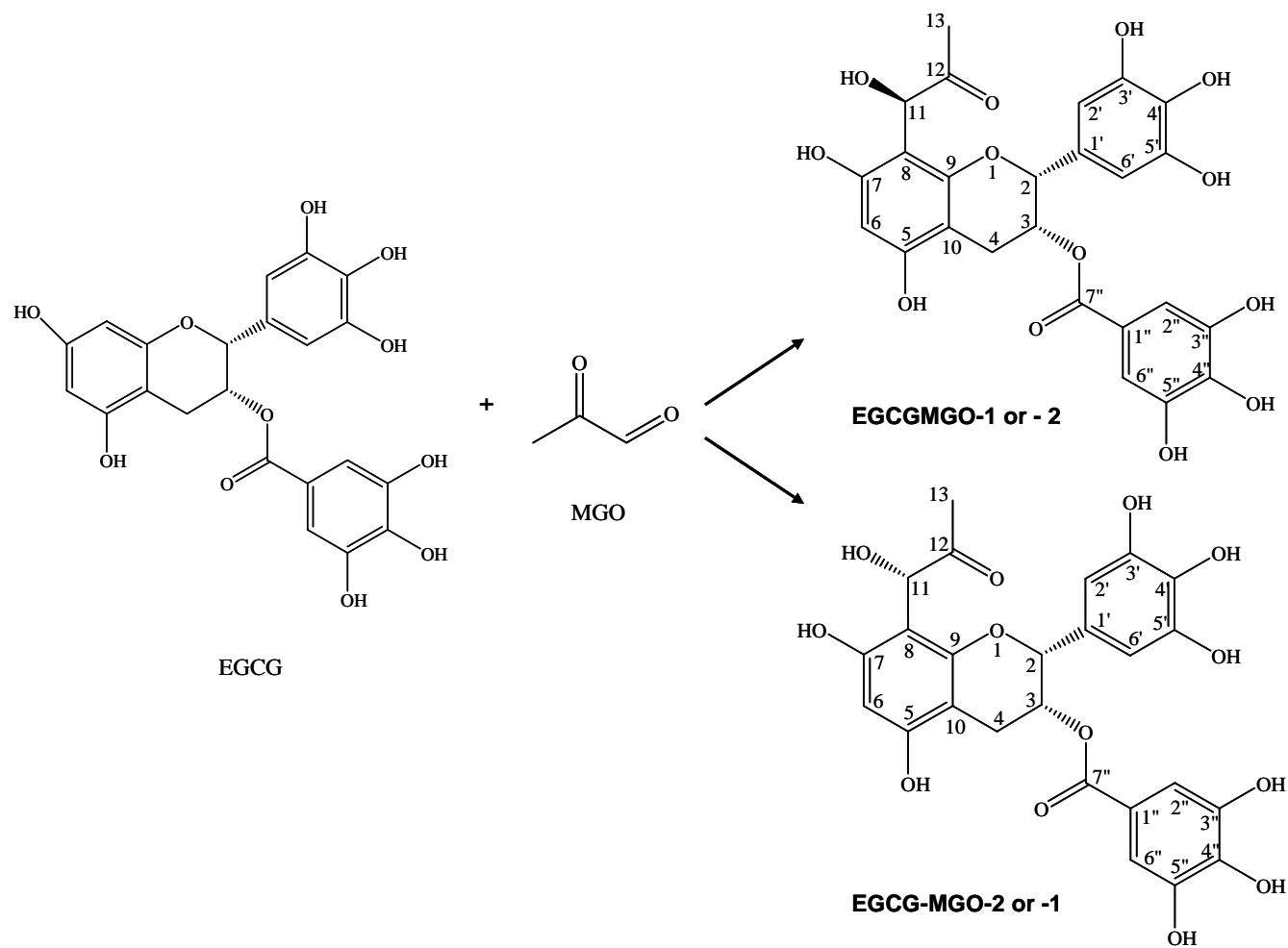


Figure 24.  $^1\text{H}$ -NMR spectrum of EGCGMGO-1

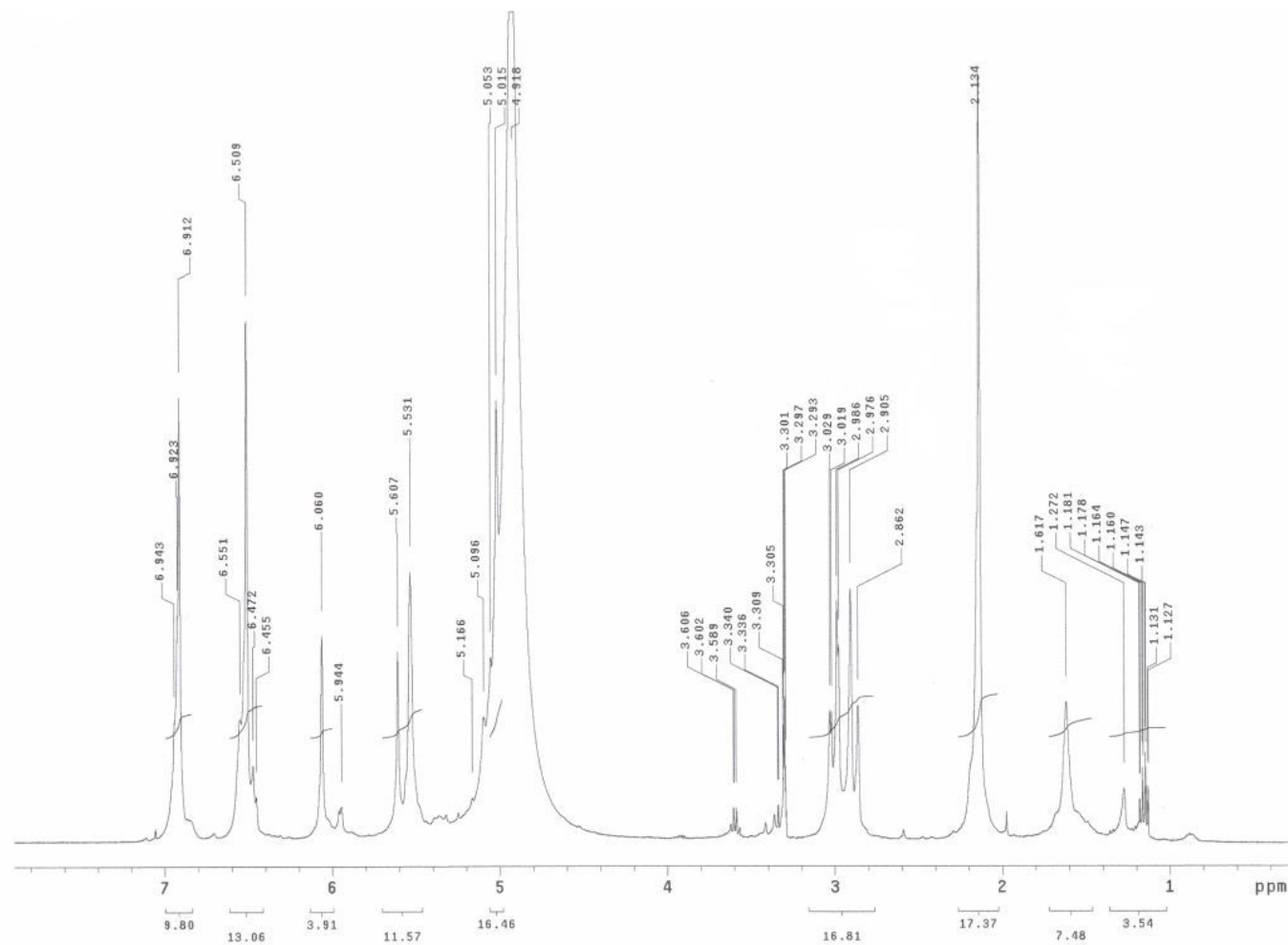
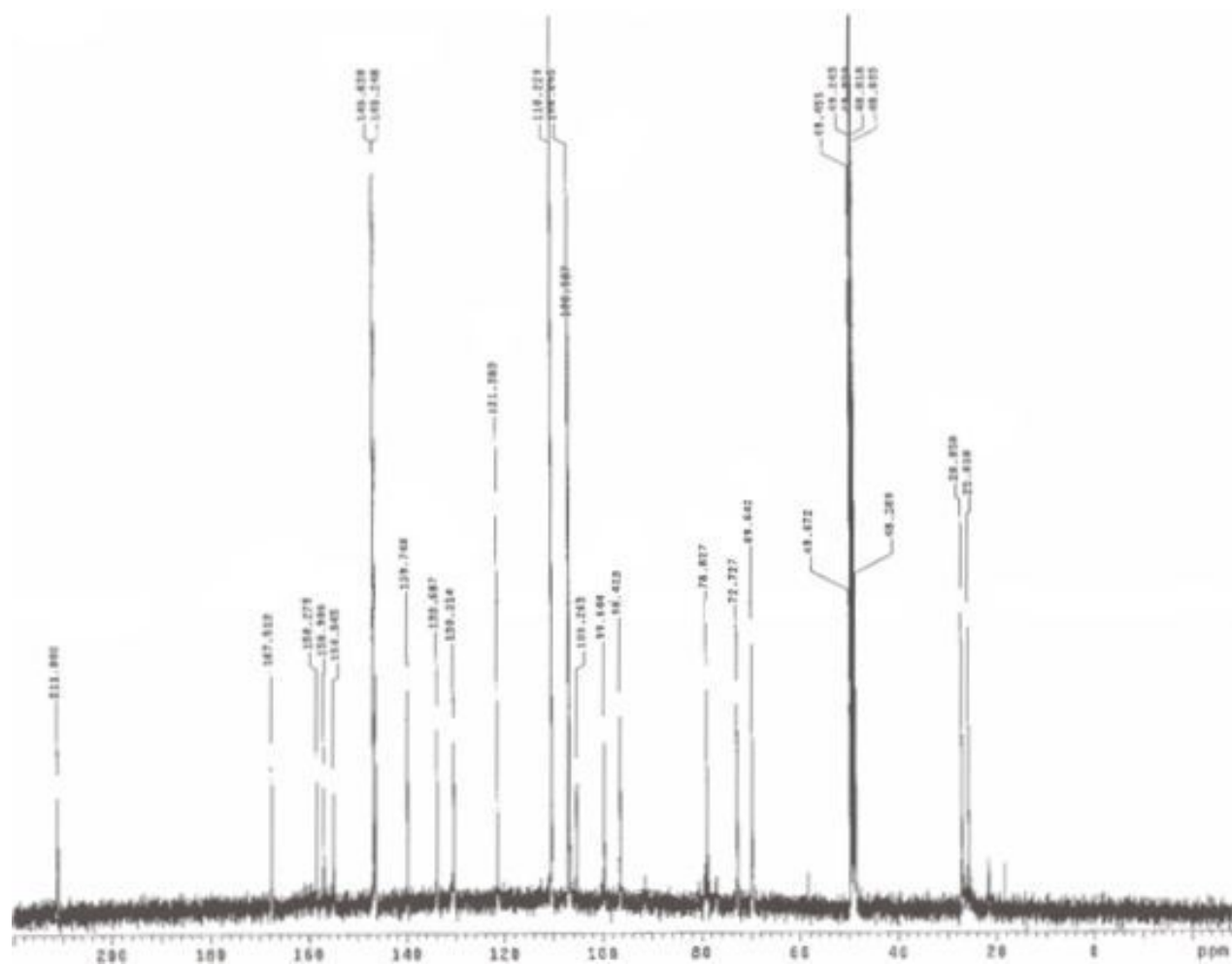
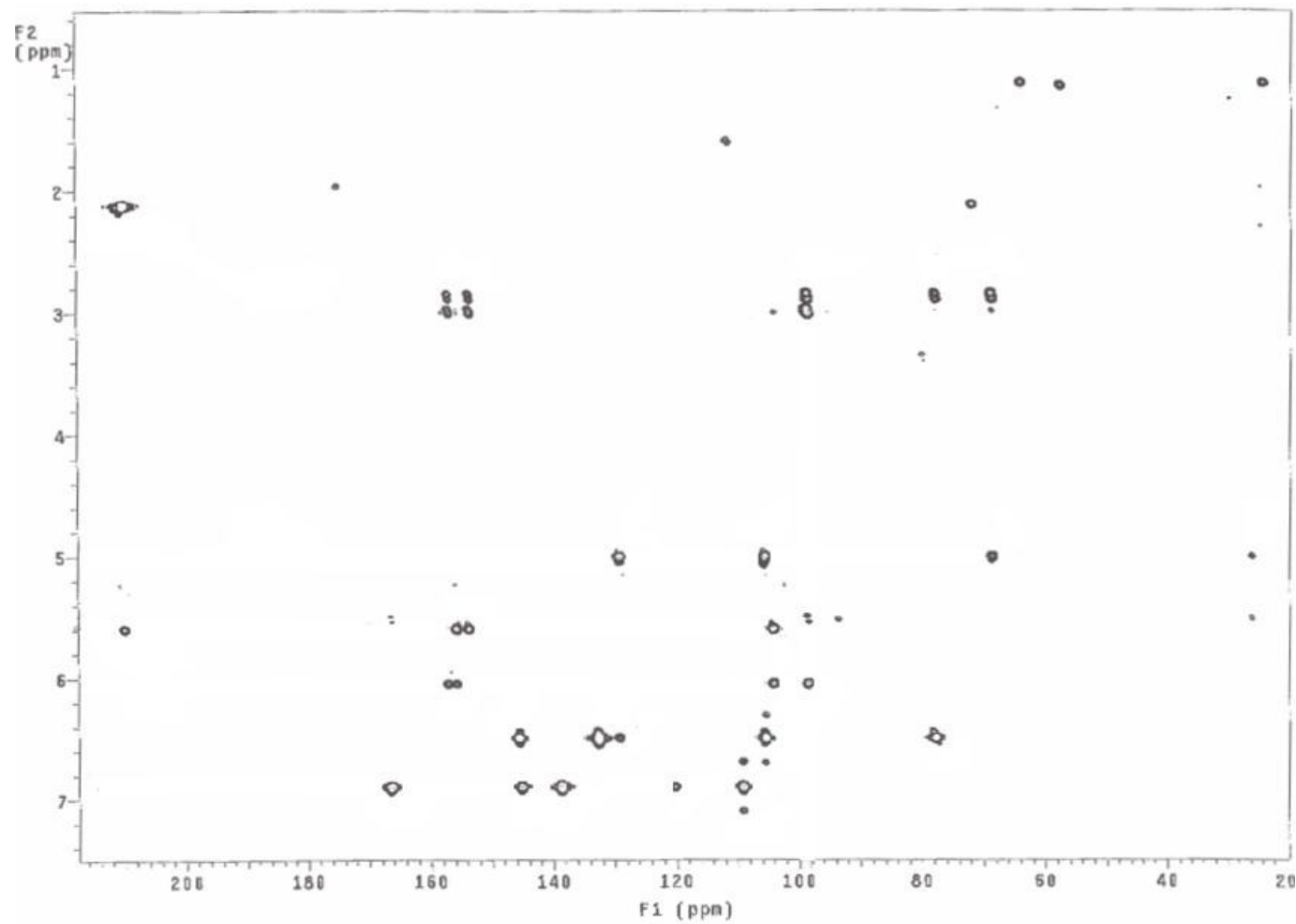


Figure 25.  $^{13}\text{C}$ -NMR spectrum of EGCGMGO-1

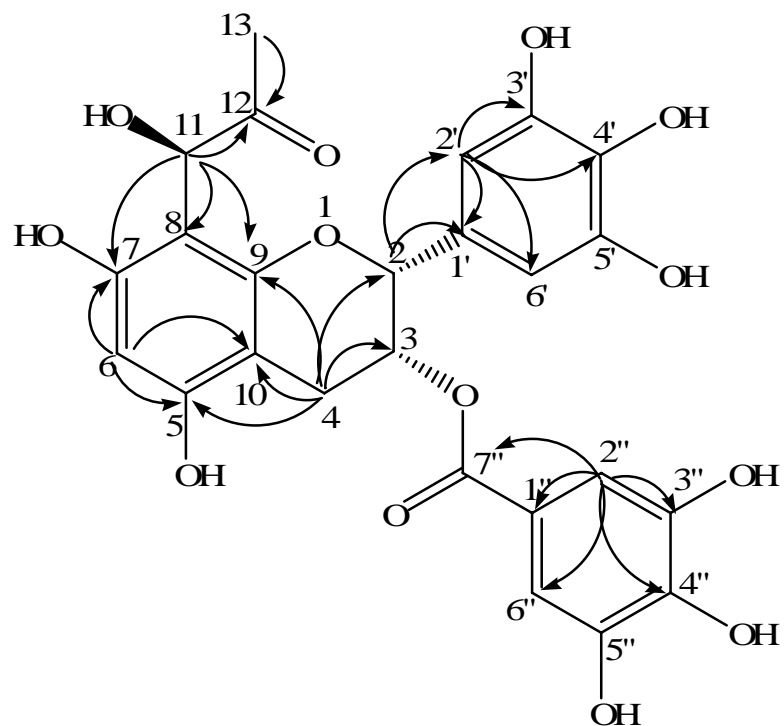


**Figure 26. HMBC (Heteronuclear Multiple Bond Correlation) spectrum of EGCGMGO-1**

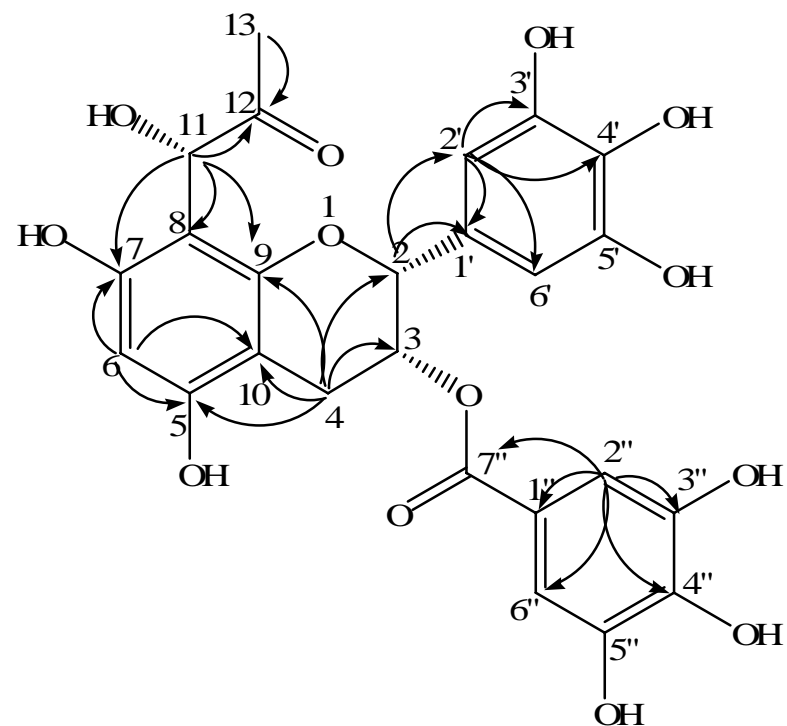




**Figure 27. Significant HMBC (H-C) correlations of EGCGMGO-1 and EGCGMGO-2**



**EGCGMGO-1 or -2**



**EGCGMGO-2 or -1**

**Figure 28. HMQC (Heteronuclear Multiple Quantum Correlation) spectrum of EGCGMGO-1**

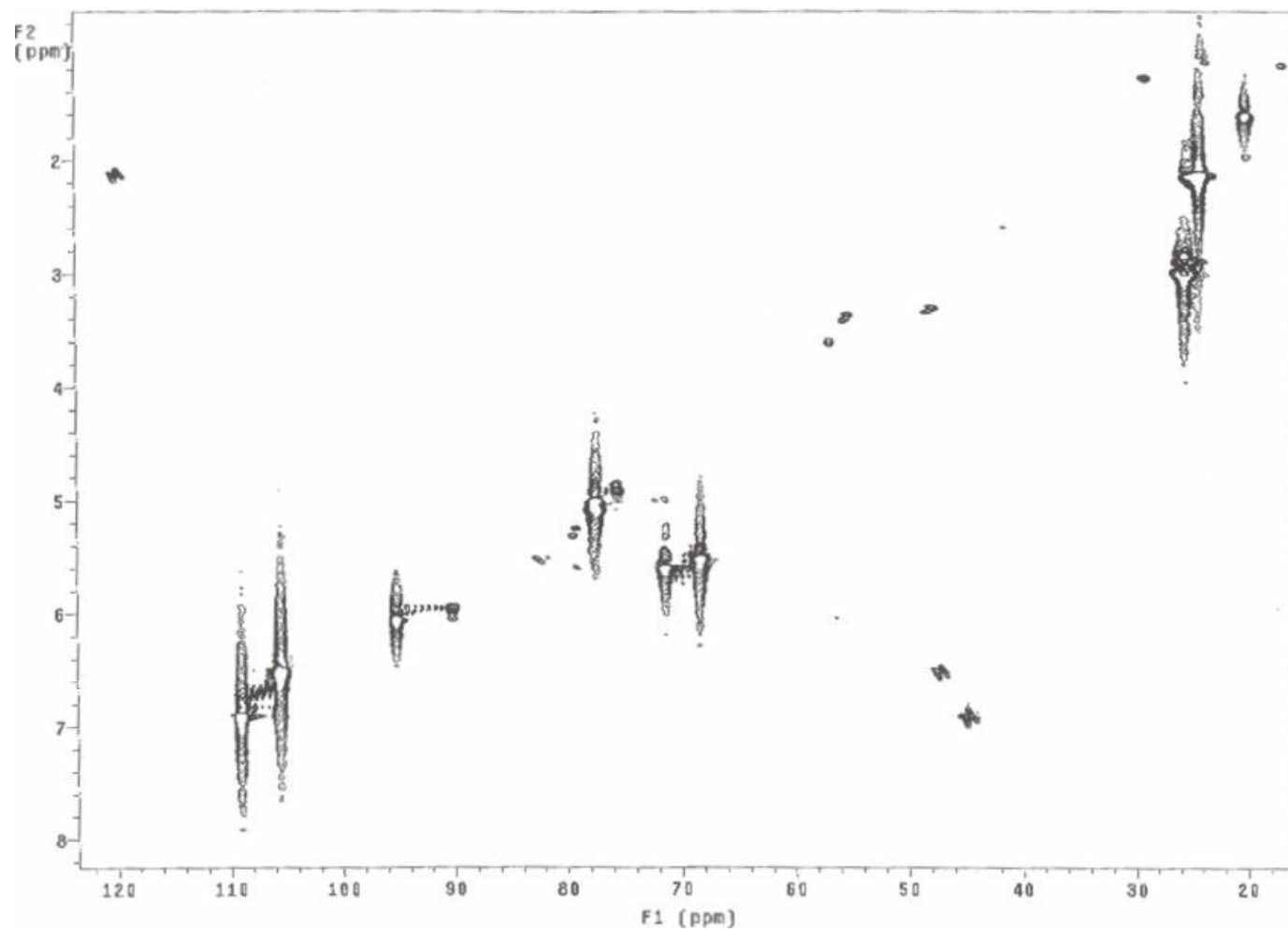


**Figure 29.**  $^1\text{H}$ -NMR spectrum of EGCGMGO-2

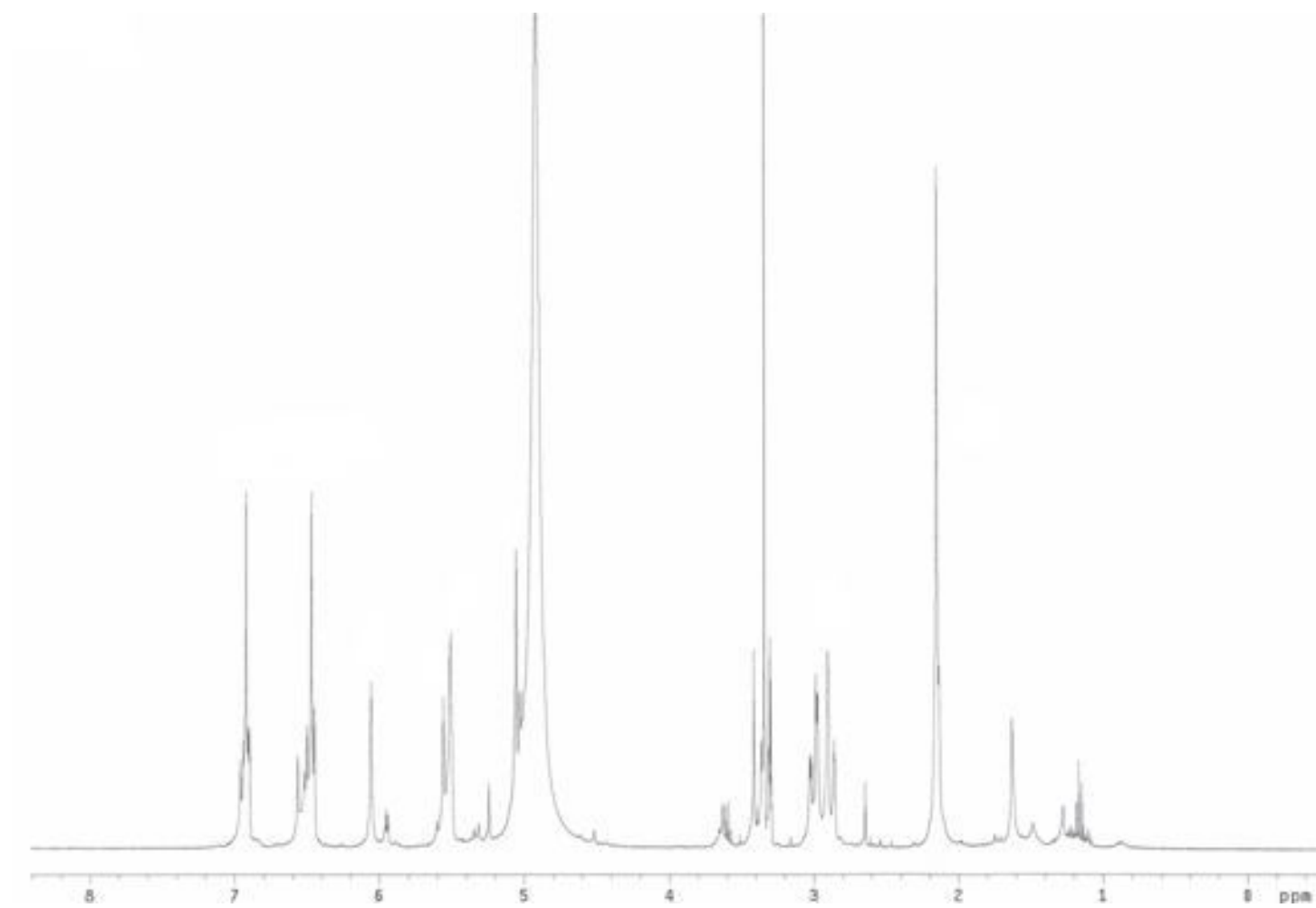


Figure 30.  $^{13}\text{C}$ -NMR spectrum of EGCGMGO-2

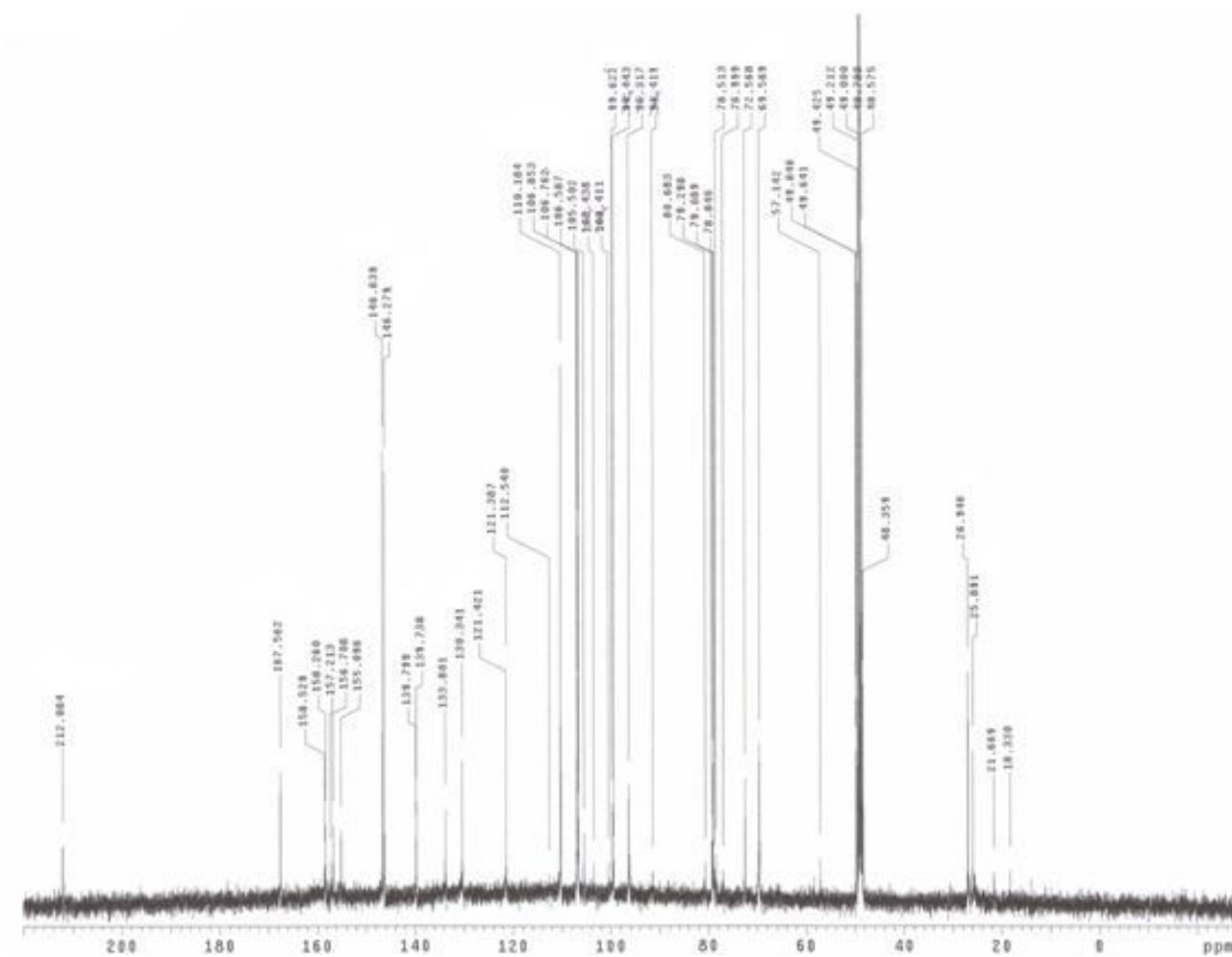


Figure 31. HMBC (Heteronuclear Multiple Bond Correlation) spectrum of EGCGMGO-2

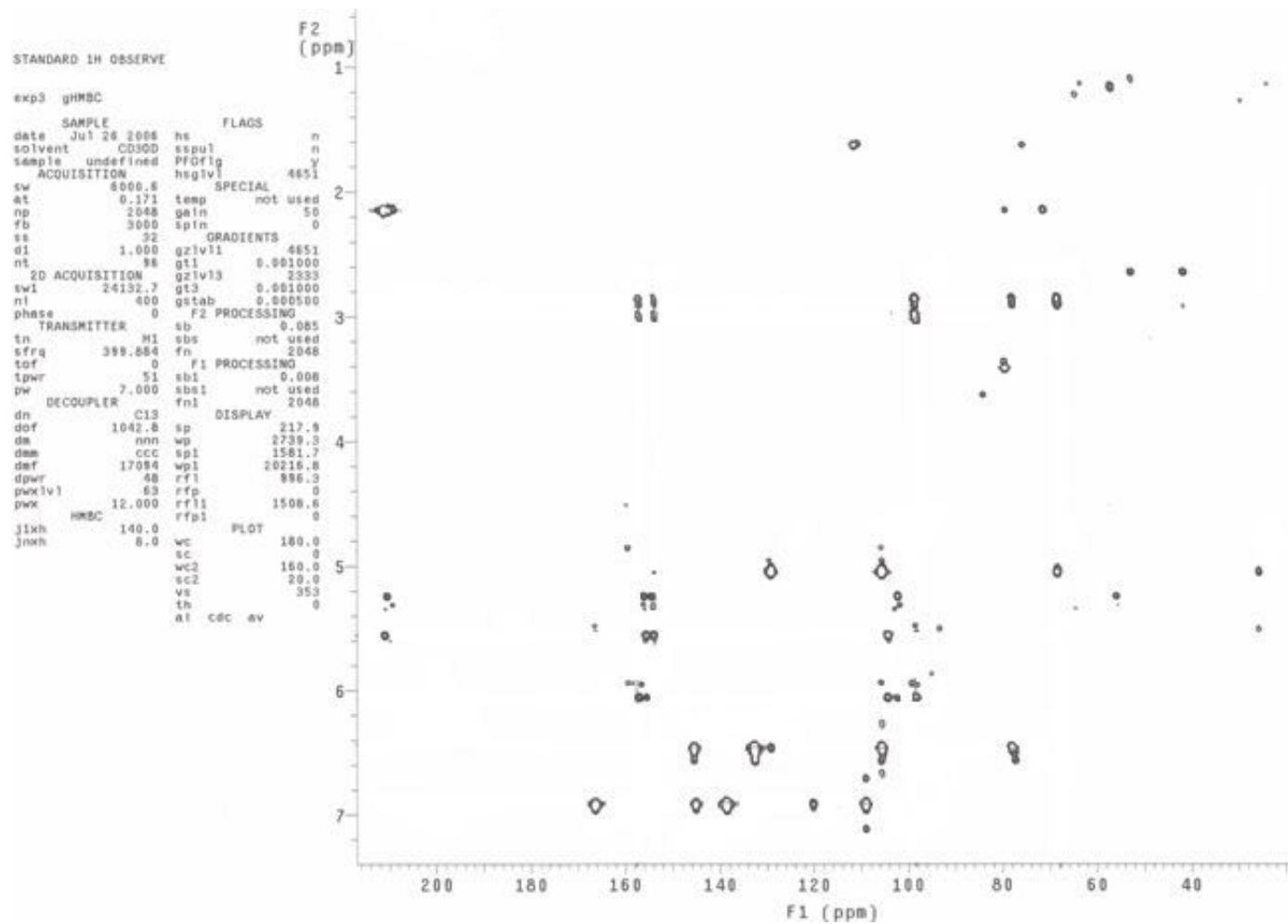
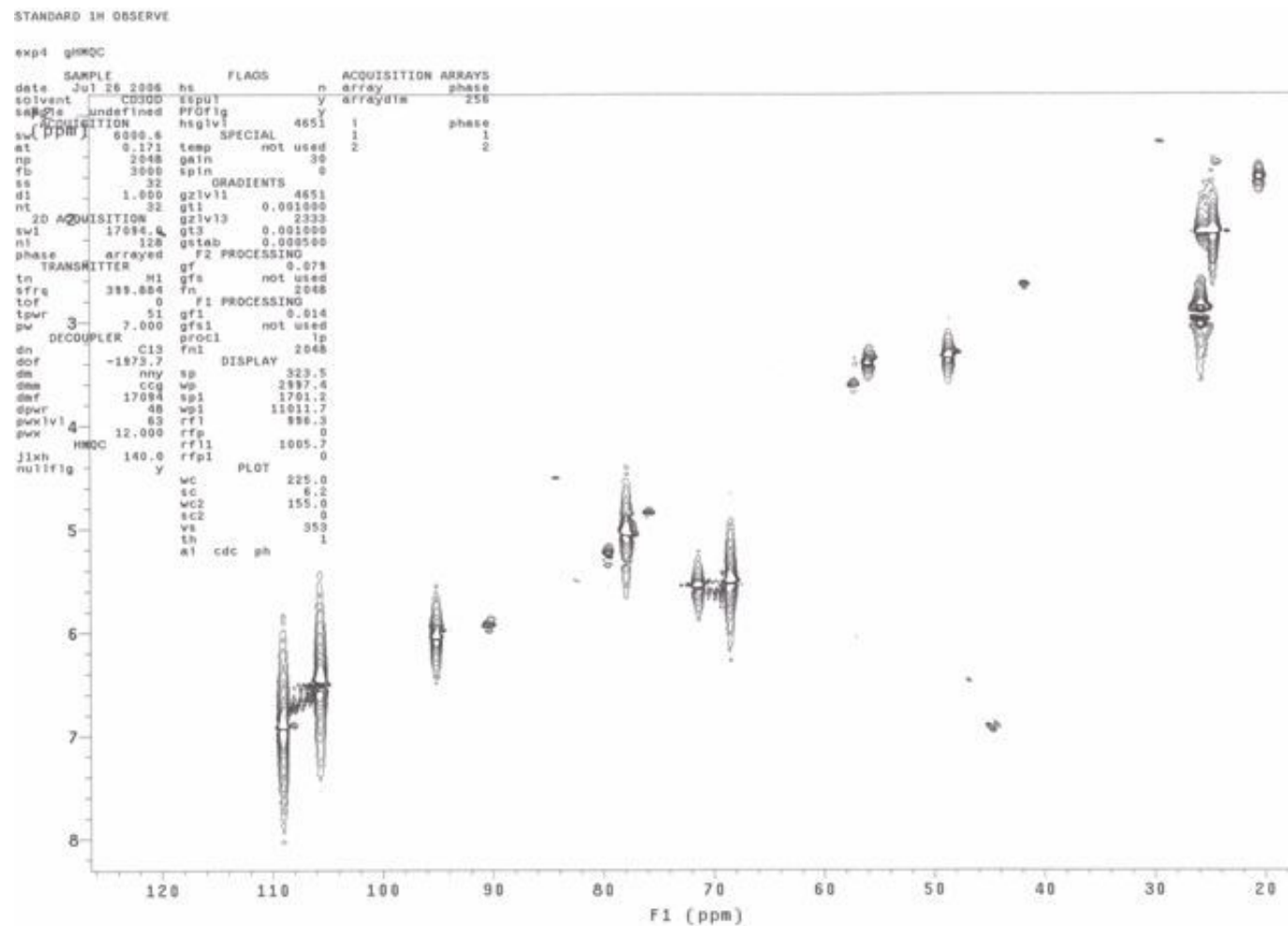


Figure 32. HMQC (Heteronuclear Multiple Quantum Correlation) spectrum of EGCGMGO-2



## References

- Ahmed, M.; Thorpe, S.R.; Baynes, J.W. Identification of N(ε)-carboxymethyllysine as a degradation product of fructoselysine in glycated protein. *J. Biol. Chem.* 1986, 61, 4889-4894.
- Akira, K.; Matsumoto, Y.; Hashimoto, T. Determination of urinary glyoxal and methylglyoxal by high-performance liquid chromatography. *Clin Chem Lab Med.* 2004, 42, 147-153.
- Annunziata, L.; Riccardo, F.; Antonio, D.V.; Antonella, S.; Rachele, R.; Domenico, F.; Elisa, B.; Roberta, S.; Pietro, P. Glyoxal and methylglyoxal levels in diabetic patients: Quantitative determination by a new GC/MS method. *Clinical Chemistry and Laboratory Medicine.* 2003, 41(9), 1166-1173.
- Barrenscheen, H.K.; Braun, K. Farb-und Fällungsreaktionen des Methylglyoxals. *Biochem. Zeitsch.* 1931, 233, 296-304.
- Bednarski, W.; Jedrychowski, L.; Hammond, E.G.; Nikolov, Z.L. A method for the determination of α-dicarbonyl compounds. *J. Dairy Sci.* 1989, 72, 2474-2477.
- Beisswenger, P.J.; Szwegold, B.S. α-Oxoaldehyde metabolism and diabetic complications, *Biochemical Society Transactions.* 2003, 31, 1358-1363.
- Beisswenger, P.; Ruggiero-Lopez, D. Metformin inhibition of glycation processes. *Diabetes Metab.* 2003, 29, 6S95-103.
- Bolton, W.K.; Cattran, D.C.; Williams, M.E.; Adler, S.G.; Appel, G.B.; Cartwright, K.; Foiles, P.G.; Freedman, B.I.; Raskin, P.; Ratner, R.E.; Spinowitz, B.S.; Whittier, F.C.; Wuerth, J.P.; ACTION I Investigator Group. Randomized trial of an inhibitor of formation of advanced glycation end products in diabetic nephropathy. *Am J Nephrol.* 2004, 24, 32-40.
- Brunner, N.A.; Henner, B.; Bettina, S.; Reinhard, Hensel. NAD<sup>+</sup>-dependent glyceraldehyde-3-phosphate dehydrogenase from *Thermoproteus tenax*. The first identified archaeal member of the aldehyde dehydrogenase superfamily is a glycolytic enzyme with unusual regulatory properties. *J. Biol. Chem.* 1998, 273, 18714-18719.
- Bucala, R.; Vlassara, H. Advanced glycosylation endproducts in diabetic renal disease: clinical measurement, pathophysiological significance, and prospects for pharmacological inhibition. *Blood Purif.* 1995, 13, 160-70.
- Casazza, J.P.; Felver, M.E.; Veech, R.L. The metabolism of acetone in rat. *J. Biol.*

*Chem.* 1984, 259, 231-236.

- Chaplen, F.W.R.; Fahl, W.E.; Cameron, D.C. Method for determination of free intracellular and extracellular methylglyoxal in animal cells grown in culture. *Analytical Biochemistry*. 1996, 238(2), 171-178.
- Creighton, D.J.; Guha, M.K. Diffusion-dependent rates for the hydrolysis reaction catalyzed by glyoxalase II from rat erythrocytes. *Biochemistry*. 1988, 27, 7376-7384.
- Daniel, R.L.; Marc, L.; Gerard, M.; Gerard, P.; Michel, L.; Nicolas, W. Reaction of metformin with dicarbonyl compounds. Possible implication in the inhibition of advanced glycation end product formation. *Biochemical Pharmacology*. 1999, 58, 1765-1773.
- DeGroot, J.; Verzijl, N.; Budde, M.; Bijlsma, J.W.; Lefeber, F.P.; TeKoppele, J.M. Accumulation of advanced glycation end products decreases collagen turnover by Bovine chondrocytes. *Experimental Cell Research*. 2001, 266, 303-310.
- Edelstein, D.; Brownlee, M. Mechanistic studies of advanced glycosylation end product inhibition by aminoguanidine. *Diabetes*. 1992, 41, 26-29.
- Espinosa-Mansilla, A.; Duran, M.I.; Salinas, F. High-performance liquid chromatographic-fluorometric determination of glyoxal, methylglyoxal, and diacetyl in urine by prederivatization to pteridinic rings. *Anal Biochem*. 1998, 255, 263-73.
- Fang, X.; Qiu, F.; Yan, B.; Wang, H.; Mort, A.J.; Stark, R.E. NMR studies of molecular structure in fruit cuticle polyesters. *Phytochemistry*. 2001, 57, 1035-1042.
- Fujioka, K.; Shibamoto, T. Formation of genotoxic dicarbonyl compounds in dietary oils upon oxidation. *Lipids*. 2004, 39, 481-486.
- Golej, J.; Hoeger, H.; Radner, W.; Unfried, G.; Lubec, G. Oral administration of methylglyoxal leads to kidney collagen accumulation in the mouse, *Life Sciences*. 1998, 63, 801-807.
- Gugliucci, A. Glycation as the glucose link to diabetic complications. *J Am Osteopath Assoc*. 2000, 100, 621-634.
- Hakim, I.A.; Alsaif, M.A.; Alduwaihy, M.; Al-Rubeaan, K.; Al-Nuaim, A.R.; Al-Attas, O.S. Tea consumption and the prevalence of coronary heart disease in



Saudi adults: results from a Saudi national study. *Prev Med.* 2003, 36(1), 64-70.

- Halliwell, B.; Chirico, S. Lipid peroxidation: its mechanism, measurement, and significance. *Am J Clin Nutr.* 1993, 57, 715s-725s.
- Hiroshi, T.; Mitsuyo, I.; Miki, T.; Wu J.B.; Toshiyasu, B.; Ikuko, K. Effect of green tea on blood glucose levels and serum proteomic patterns in diabetic (db/db) mice and on glucose metabolism in healthy humans. *BMC pharmacology.* 2004, 4:18.
- Hollnagel, A.; Kroh, L.W.; Formation of a-dicarbonyl fragments from mono- and disaccharides under caramelization and Maillard reaction conditions, *Lebensm. Unters. Forsch. A.* 1998, 207, 50-54.
- Jakus, V.; Rietbrock, N. Advanced glycation end-products and the progress of diabetic vascular complications. *Physiol Res.* 2004, 53, 131-142.
- Kalapos, M.P. Methylglyoxal in living organisms: Chemistry, biochemistry, toxicology and biological implications, *Toxicology letters.* 1999, 110, 145-175.
- Kao, Y.H.; Hiipakka, R.A.; Liao, S. Modulation of endocrine systems and food intake by green tea epigallocatechin gallate. *Endocrinology.* 2000, 141(3), 980-7.
- Kazuaki, H.; Wang, M.F.; Liao, M.L.; Chuang, C.K.; Miyuki, I.; Clevidence, B.; Yamamoto, S. Antihyperglycemic effect of oolong tea in type 2 diabetes. *Diabetes Care.* 2003, 26(6), 1714-1718.
- Lederer, M.O.; Klaiber, R.G.B. Cross-linking of proteins by Maillard processes: characterization and detection of lysine-arginine cross-links derived from glyoxal and methylglyoxal. *Med. Chem.* 1999, 7, 2499-2507.
- Lo, C.Y.; Li, S.; Tan, D.; Pan, M.H.; Sang, S.; Ho, C.T. Trapping reactions of reactive carbonyl species with tea polyphenols in simulated physiological conditions. *Mol Nutr Food Res.* 2006, 50, 1118-1128.
- Lo, T.W.; Selwood, T.; Thornalley, P.J. The reaction of methylglyoxal with aminoguanidine under physiological conditions and prevention of methylglyoxal binding to plasma proteins. *Biochem Pharmacol.* 1994, 48, 1865-1870.
- Lyles, G.A.; Singh, I. The metabolism of aminoacetone to methylglyoxal by semicarbazide-sensitive amine oxidase in human umbilical artery. *Biochem. Pharmacol.* 1992, 43, 1409-1414.
- Marins, S.I.F.S.; van Boekel, M.A.J.S. Kinetic modelling of Amadori N-(1-

deoxy-D-fructos-1-yl)-glycine degradation pathways. *Carbohydr. Res.* 2003, 338, 1651-1663.

- Mclellan, A.C.; Phillips, S.A.; Thornalley, P.J. Fluorometric assay of D-lactate. *Anal. Biochem.* 1992, 206, 17-23.
- Michael, J.; Roberts, G.T.; Wondrak, D.C.L.; Jacobson, M.K.; Jacobson, E.L. DNA damage by carbonyl stress in human skin cells, *Mutation Research*, 2003, 522, 45-56.
- Michiyo, H.; Tetsuya, H.; Sachiko, K.; Naohide, K.; Yasuhiko, I. Renoprotective effects of tea catechin in streptozotocin- induced diabetic rats. *International Urology and Nephrology*. 2006, 38(3-4), 693-699.
- Miyata, T.; Ueda, Y.; Shinzato, T.; Iida, Y.; Tanaka, S.; Kurokawa, K.; Maeda, K. Accumulation of albumin-linked and free-form pentosidine in the circulation of uremic patients with end-stage renal failure: renal implications in the pathophysiology of pentosidine. *J. Am. Soc. Nephrol.* 1996, 7, 1198-1206.
- Miyata, T.; Sugiyama, S.; Saito, A.; Kurokawa, K. Reactive carbonyl compounds related uremic toxicity ("carbonyl stress"). *Kidney Int Suppl.* 2000, 78, 25-31.
- Nagaraj, R.H.; Sarkar, P.; Mally, A.; Biemel, K.M.; Lederer, M.O.; Padayatti, P. S. Effect of pyridoxamine on chemical modification of proteins by carbonyls in diabetic rats: characterization of a major products from the reaction of pyridoxamine and methylglyoxal. *Arch Biochem Biophys.* 2002, 402, 110-119.
- Natsuki, M.; Fumiko, I.; Akiyo, I.; Hirotooshi, I.; Yukihiro, H. Reduction of blood glucose levels by tea catechins. *Bioscience, Biotechnology, and Biochemistry*. 1993, 57(4), 525-7.
- Nemet, I.; Lidiya, V.D.; Zdenka, T. Preparation and quantification of methylglyoxal in human plasma using reverse-phase high-performance liquid chromatography. *Clinical Biochemistry*. 2004, 37, 875-881.
- Nemet, I.; Turk, Z. Review: Methylglyoxal in food and living organisms, *Mol. Nutr. Food Res.* 2006, 50, 1105-1117.
- Nemet, I.; Varga-Defterdarovic, L.; Zdenka, T. Review: Methylglyoxal in food and living organisms. *Mol. Nutr. Food Res.* 2006, 50, 1105-1117.
- Nemet, I.; Varga-Defterdarovic, L.; Turk, Z. Preparation and quantification of methylglyoxal in human plasma using reverse-phase high-performance liquid chromatography. *Clin Biochem.* 2004, 37, 875-881.

- Nicholl, I.D.; Bucala, R. Advanced glycation end products and cigarette smoking. *Cell. Mol. Biol.* 1998, 44, 1025-1033.
- Odani, H.; Shinzato, T.; Matsumoto, Y.; Usami, J.; Maeda, K. Increase in three alpha, beta-dicarbonyl compound levels in human uremic plasma: specific *in vivo* determination of intermediates in advanced Maillard reaction. *Biochem Biophys Res Commun.* 1999, 256, 89-93.
- Paul, R.G.; Avery, N.C.; Slatter, D.A.; Sims, T.J.; Bailey, A.J. Isolation and characterization of advanced glycation end products derived from the *in vitro* reaction of ribose and collagen. *Biochem. J.* 1998, 330, 1241-1248.
- Ping, O.Y.; Peng, W.L.; Xu, D.L.; Lai, W.Y.; Xu, A.L. Green tea polyphenols inhibit advanced glycation end product-induced rat vascular smooth muscle cell proliferation. *Di Yi Junyi Daxue Xuebao.* 2004, 24(3), 247-251.
- Pompliano, D.L.; Peyman, A.; Knowles, J.R. Stabilization of a reaction intermediate as a catalytic device: definition of the functional role of the flexible loop in triosephosphate isomerase. *Biochemistry.* 1990, 29, 3186-3194.
- Randell, E.W.; Vasdev, S.; Gill, V. Measurement of methylglyoxal in rat tissues by electrospray ionization mass spectrometry and liquid chromatography. *Journal of Pharmacological and Toxicological Methods.* 2005, 51, 153-157.
- Revel, G.D.; Pripis-Nicolau, L.; Barbe, J.C.; Bertrand, A. The detection of  $\alpha$ -dicarbonyl compounds in wine by formation of quinoxaline derivatives. *J. Sci. Food Agric.* 2000, 80, 102-108.
- Richard, J.P. Mechanism for the formation of methylglyoxal from triosephosphates. *Biochem. Soc. Trans.* 1993, 21, 549-537.
- Rutter, K.; Sell, D.R.; Fraser, N.; Obrenovich, M.; Zito, M.; Starke-Reed, P.; Monnier, V.M. Green tea extract suppresses the age-related increase in collagen crosslinking and fluorescent products in C57BL/6 mice. *Int J Vitam Nutr Res.* 2003, 73, 453-460.
- EUROPEAN COMMISSION, SCIENTIFIC COMMITTEE ON CONSUMER PRODUCTS (SCCP) opinion on Glyoxal, the 4<sup>th</sup> plenary of June 2005, [http://ec.europa.eu/health/ph\\_risk/committees/04\\_sccp/docs/sccp\\_o\\_023.pdf](http://ec.europa.eu/health/ph_risk/committees/04_sccp/docs/sccp_o_023.pdf)
- Singh, R.; Barden, A.; Mori, T.; Beilin, L. Advanced glycation end-products: a review. *Diabetologia*, 2001, 44, 129-146.

- Stadler, K.; Jenei, V.; Somogyi, A.; Jakus, J. Beneficial effects of aminoguanidine on the cardiovascular system of diabetic rats. *Diabetes Metab Res Rev.* 2005, 21, 189-196.
- Vlassara, H. Advanced glycation in diabetic renal and vascular disease. *Kidney Int Suppl.* 1995, 51, S43-44.
- Yamabe, N.; Yokozawa, T.; Oya, T.; Kim, M.J. Therapeutic potential of (-)-Epigallocatechin 3-O-Gallate on renal damage in diabetic nephropathy model rats. *JPET.* 2006, 319, 228-236.
- Yang, C.S.; Lee, M.J.; Chen, L.; Yang, G.Y. Polyphenols as Inhibitors of Carcinogenesis. *Environmental Health Perspectives.* 1997, 105, Supplement 4.
- Yim, M.B.; Yim, H.S.; Lee, C.; Kang, S.O.; Chock, P.B. Protein glycation: creation of catalytic sites for free radical generation. *Ann. N. Y. Acad. Sci.* 2001, 928, 48-53.
- Wu, C.H.; Yen, G.C. Inhibitory effect of naturally occurring flavonoids on the formation of advanced glycation endproducts. *Journal of agricultural and food chemistry.* 2005, 53(8), 3167-73.